

# EMT Inducers Catalyze Malignant Transformation of Mammary Epithelial Cells and Drive Tumorigenesis towards Claudin-Low Tumors in Transgenic Mice

Anne-Pierre Morel<sup>1,2,3,4,5,6,9</sup>, George W. Hinkal<sup>1,2,3,4,5,6,9</sup>, Clémence Thomas<sup>1,2,3,4,5,6,9</sup>,  
Frédérique Fauvet<sup>1,2,3,4,5,6</sup>, Stéphanie Courtois-Cox<sup>1,2,3,4,5,6</sup>, Anne Wierinckx<sup>1,2,3,4,5,7</sup>,  
Mojgan Devouassoux-Shisheboran<sup>1,2,3,4,5,8</sup>, Isabelle Treilleux<sup>1,2,4,6</sup>, Agnès Tissier<sup>1,2,3,4,5,6</sup>,  
Baptiste Gras<sup>1,2,3,4,5,6</sup>, Julie Pourchet<sup>1,2,3,4,5,6</sup>, Isabelle Puisieux<sup>1,2,3,4,5,6</sup>, Gareth J. Browne<sup>9</sup>,  
Douglas B. Spicer<sup>10</sup>, Joël Lachuer<sup>1,2,3,4,5,7</sup>, Stéphane Ansieau<sup>1,2,3,4,5,6\*</sup>, Alain Puisieux<sup>1,2,3,4,5,6,11\*</sup>

**1** Inserm UMR-S1052, Centre de Recherche en Cancérologie de Lyon, Lyon, France, **2** CNRS UMR5286, Centre de Recherche en Cancérologie de Lyon, Lyon, France, **3** LabEx DEVweCAN, Lyon, France, **4** UNIV UMR1052, Centre de Recherche en Cancérologie de Lyon, Lyon, France, **5** Université de Lyon, Lyon, France, **6** Centre Léon Bérard, Lyon, France, **7** ProfileXpert, Bron, France, **8** Hôpital de la Croix-Rousse, Lyon, France, **9** Department of Cancer Studies and Molecular Medicine, University of Leicester, Leicester, United Kingdom, **10** Center for Molecular Medicine, Maine Medical Center Research Institute, Scarborough, Maine, United States of America, **11** Institut Universitaire de France, Paris, France

## Abstract

The epithelial-mesenchymal transition (EMT) is an embryonic transdifferentiation process consisting of conversion of polarized epithelial cells to motile mesenchymal ones. EMT-inducing transcription factors are aberrantly expressed in multiple tumor types and are known to favor the metastatic dissemination process. Supporting oncogenic activity within primary lesions, the TWIST and ZEB proteins can prevent cells from undergoing oncogene-induced senescence and apoptosis by abolishing both p53- and RB-dependent pathways. Here we show that they also downregulate PP2A phosphatase activity and efficiently cooperate with an oncogenic version of H-RAS in malignant transformation of human mammary epithelial cells. Thus, by down-regulating crucial tumor suppressor functions, EMT inducers make cells particularly prone to malignant conversion. Importantly, by analyzing transformed cells generated *in vitro* and by characterizing novel transgenic mouse models, we further demonstrate that cooperation between an EMT inducer and an active form of RAS is sufficient to trigger transformation of mammary epithelial cells into malignant cells exhibiting all the characteristic features of claudin-low tumors, including low expression of tight and adherens junction genes, EMT traits, and stem cell-like characteristics. Claudin-low tumors are believed to be the most primitive breast malignancies, having arisen through transformation of an early epithelial precursor with inherent stemness properties and metaplastic features. Challenging this prevailing view, we propose that these aggressive tumors arise from cells committed to luminal differentiation, through a process driven by EMT inducers and combining malignant transformation and transdifferentiation.

**Citation:** Morel A-P, Hinkal GW, Thomas C, Fauvet F, Courtois-Cox S, et al. (2012) EMT Inducers Catalyze Malignant Transformation of Mammary Epithelial Cells and Drive Tumorigenesis towards Claudin-Low Tumors in Transgenic Mice. *PLoS Genet* 8(5): e1002723. doi:10.1371/journal.pgen.1002723

**Editor:** Marshall S. Horwitz, University of Washington, United States of America

**Received:** November 18, 2011; **Accepted:** April 2, 2012; **Published:** May 24, 2012

**Copyright:** © 2012 Morel et al. This is an open-access article distributed under the terms of the Creative Commons Attribution License, which permits unrestricted use, distribution, and reproduction in any medium, provided the original author and source are credited.

**Funding:** Our team is labeled by the Ligue Nationale contre le Cancer. The work was additionally supported by the Ligue Nationale contre le Cancer (Comité de l'Ain), the Institut National contre le Cancer (project PLBI009), the Project National Cancer Association, and by institutional grants from the LabEX DEVweCAN (ANR-10-LABX-61). GWH and SC-C were recipients of fellowships from the INCa (Project 07/3D1616/PL-969-017/NG-NC) and the Fondation de France (Project 2007 005222), respectively. CT was first granted by a Cifre (INSERM-Centre Léon Bérard) fellowship and next a recipient of fellowships of the Association pour la Recherche sur le Cancer (ARC). The funders had no role in study design, data collection and analysis, decision to publish, or preparation of the manuscript.

**Competing Interests:** The authors have declared that no competing interests exist.

\* E-mail: stephane.ansieau@lyon.unicancer.fr (SA); alain.puisieux@lyon.unicancer.fr (AP)

† These authors contributed equally to this work.

## Introduction

While the disruption of embryonic processes has been acknowledged as a cause of the outgrowth of paediatric neoplasms, more recent observations suggest that the aberrant reactivation of developmental regulatory programs might also contribute to progression in the advanced stages of cancers in adults [1]. At the crux of this concept is the subversion of the epithelial-mesenchymal transition (EMT) during tumor progression. This developmental program converts epithelial cells into mesenchymal ones through profound disruption of cell-cell junctions, loss of

apical-basolateral polarity and extensive reorganization of the actin cytoskeleton [2]. During embryogenesis, EMT plays critical roles in the formation of the body plan and in the differentiation of most of the tissues and organs derived from the mesoderm and the endoderm [3]. This process is tightly regulated through a delicate interplay between environmental signals from WNT, TGF $\beta$ , FGF family members, and a complex network of signaling pathways that converge on the activation of transcription factors that induce EMT through repression of *CDH1* (encoding for the E-cadherin) and activation of mesenchymal genes. EMT-inducing transcription factors include several zinc finger proteins (e.g., SNAIL1,

## Author Summary

The epithelial-mesenchymal transition (EMT) is essential to germ layer formation and cell migration in the early vertebrate embryo. EMT is aberrantly reactivated under pathological conditions, including fibrotic disease and cancer progression. In the latter process, EMT is known to promote invasion and metastatic dissemination of tumor cells. EMT is orchestrated by a variety of embryonic transcription factors called EMT inducers. Among these, the TWIST and ZEB proteins are known to be frequently reactivated during tumor development. We here report *in vitro* and *in vivo* observations demonstrating that activation of these factors fosters cell transformation and primary tumor growth by alleviating key oncosuppressive mechanisms, thereby minimizing the number of events required for acquisition of malignant properties. In a model of breast cancer, cooperation between a single EMT inducer and a single mitogenic oncoprotein is sufficient to transform mammary epithelial cells into malignant cells and to drive the development of aggressive and undifferentiated tumors. Overall, these data underscore the oncogenic role of embryonic transcription factors in initiating the development of poor-prognosis neoplasms by promoting both cell transformation and dedifferentiation.

SNAIL2), basic helix-loop-helix transcription factors (e.g., TWIST1, TWIST2 and E2A) and zinc-finger and homeodomain proteins (ZEB1, ZEB2/SIP1) [4,5]. Importantly, while EMT inducers are maintained in a silent state in adult differentiated epithelial cells, their reactivation is commonly observed in a variety of human cancers with a frequent correlation with poor clinical outcome [6]. In the course of tumor progression, the gain of cell motility and the secretion of matrix metalloproteases associated with EMT promote cancer cell migration across the basal membrane and invasion of the surrounding microenvironment, favoring metastatic dissemination. Furthermore, EMT may also facilitate second site colonization by endowing cells with stem-like features including self-renewing properties [7–9]. While the involvement of EMT inducers in the invasion-metastasis cascade of epithelial tumors is well delineated, their contribution to tumorigenesis remains unclear. Supporting an oncogenic activity within primary lesions, we recently demonstrated that the TWIST proteins were able to prevent cells from undergoing oncogene-induced senescence and apoptosis by abrogating both p53- and RB-dependent pathways [10,11]. As a consequence, TWIST1 and TWIST2 can cooperate with an activated version of RAS to transform mouse embryonic fibroblasts [11]. Furthermore, the ZEB transcription factors were recently shown to overcome EGFR-induced senescence in oesophageal epithelial cells, suggesting that several EMT-inducers might share the property of inhibiting oncogene-induced failsafe programs [12]. On the basis of these findings, we sought to formally assess the oncogenic activity of these EMT-promoting factors in the model of breast tumorigenesis by generating *Twist1* transgenic mouse models and by performing cooperation assays in human mammary epithelial cells (HMECs). The focus of this study was underpinned by the common reactivation of *ZEB1*, *ZEB2* and *TWIST1* in aggressive and undifferentiated human breast cancers, especially in the newly identified claudin-low intrinsic subtype [13]. Here we demonstrate that commitment to an EMT program favors breast tumor initiation by inhibiting crucial tumor suppressor functions, including PP2A (protein phosphatase 2A) activity, and thus minimizes the number of events required for neoplastic transfor-

mation. Importantly, upon aberrant activation of an EMT inducer, a single mitogenic activation is sufficient to transform mammary epithelial cells into malignant cells exhibiting all the characteristic features of claudin-low tumors. These findings extend our understanding of the role of EMT-inducing transcription factors during tumor development and highlight the claudin-low tumor subtype of breast cancers as the first example of human adult malignancies driven by aberrant reactivation of an embryonic transdifferentiation program.

## Results

### Twist1 expression promotes primary tumor development *in vivo*

To gain insight into the role of EMT commitment in tumor initiation and primary tumor growth, we used a *Twist1* transgenic mouse model exhibiting a lox-STOP-lox (LSL) version of the active version of the murine TWIST1 (TWIST1-E12 tethered dimer) under a ubiquitous promoter [14]. These mice were crossed with a line expressing a lox-STOP-lox regulated knock-in of the activated *K-Ras* oncogene (LSL-*K-rasG12D*) [15,16] for *in vivo* oncogenic cooperation experiments. Transgene expression was first induced using a Mouse Mammary Tumor Virus promoter driven Cre recombinase (MMTV-Cre) and thereby restricted to secretory tissues, in particular the mammary gland and skin epithelia, as well as to the hematopoietic system [17,18]. Neither wild-type nor MMTV-Cre;*Twist1* mice exhibited tumor formation by one year of age (n = 47). Expression of knock-in *K-rasG12D* was associated with low-grade splenic lymphomas as well as anal and oral papillomas (Figure 1). Importantly, papillomas never progressed to a malignant stage but could grow to the point to physical obstruction leading to cachexia and requiring euthanasia (n = 85, median survival 85 days). In contrast, MMTV-Cre;*K-rasG12D*;*Twist1* mice invariably developed aggressive multifocal squamous cell carcinomas (SCC) at very young ages necessitating euthanasia at the significantly earlier median age of 35 days (n = 12, p < 0.0001, Figure 1). These observations demonstrated for the first time the oncogenic properties of TWIST1 *in vivo* and underscored the cooperative effect between K-RAS and TWIST1 in promoting malignant conversion.

### Twist1 expression in murine differentiated mammary epithelial cells promotes the development of claudin-low breast cancers

Due to the speed with which SCC developed in the MMTV-Cre;*K-rasG12D*;*Twist1* animals, the role of TWIST1 in promoting mammary tumor formation could not be assessed. Consequently, transgene expression was next restricted to differentiated mammary epithelial cells by using mice expressing the Cre recombinase under the control of the Whey Acidic Protein promoter (WAP-Cre) [17]. WAP is a milk protein expressed late in the differentiation pathway of mammary epithelial cells [19]. The 2.6-kb fragment of the mouse WAP gene promoter used in the present study is active in the mammary alveolar epithelium during the second half of pregnancy upon the initiation of differentiation [17,20]. In virgin animals, the promoter is only transiently activated in a few mammary alveolar and ductal cells, during estrus (average age at first estrus = 35 days), allowing mosaic transgene activation so as to better mimic the emergence of spontaneous oncogenic activations [19]. Wild-type, WAP-Cre;*K-rasG12D*, and WAP-Cre;*Twist1* transgenic females exhibited normal mammary gland development (Figure 2B) and remained healthy for at least 240 days (n = 19). However, all virgin WAP-Cre;*K-rasG12D*;*Twist1* females developed multifocal breast carci-

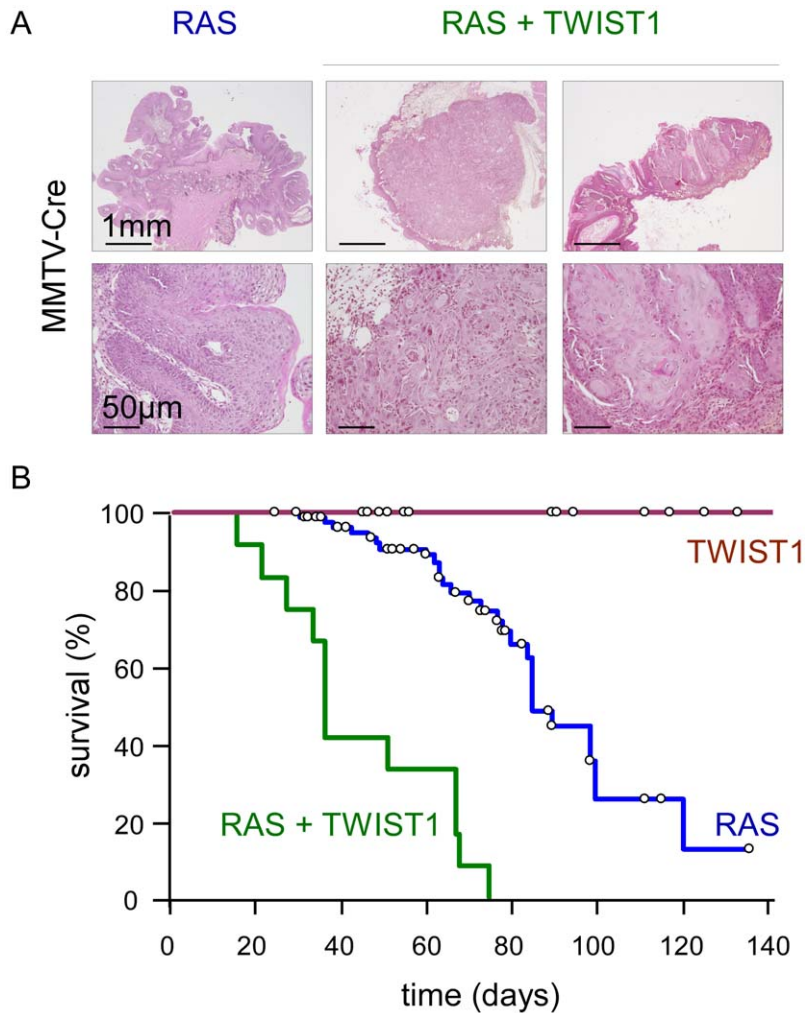


**Figure 1. Twist1 promotes tumor progression *in vivo*.** Transgene expression was driven by the MMTV-Cre. While MMTV-Cre; *Twist1* mice (TWIST1; n = 71) do not develop skin lesions, MMTV-Cre;*K-rasG12D* animals (RAS; n = 89) spontaneously develop anal and oral papillomas. In MMTV-Cre;*K-rasG12D*; *Twist1* mice (RAS+TWIST1; n = 19) papillomas evolve into squamous carcinomas. (A) HPS staining of skins either from *K-rasG12D* or *K-rasG12D*; *Twist1* transgenic mice. Transgene expression is induced by the MMTV-Cre. (B) Kaplan-Meier survival curves of transgenic mice. Survival corresponds to the end point of the experiment, the tumor burden requiring euthanasia of the animal. Open circles indicate mice censored from the dataset.

doi:10.1371/journal.pgen.1002723.g001

nomas by 140 days of age, approximately 105 days after first transgene expression ( $p < 0.001$ , median survival = 125 days, n = 9) (Figure 2A and 2D). These tumors exhibited metaplastic features with a mixed morphologic aspect that included epithelial-type and spindle shaped cells (Figure 2D). In support of the relevance of EMT *in vivo*, the presence of the tagged-TWIST1 transgene in both the epithelial and fusiform cancer cell contingents demonstrated that mesenchymal cells arose through transdifferentiation of their epithelial counterparts (Figure 2D). Molecular characterization of human and murine breast tumors led to identifying five intrinsic subtypes (luminal A, luminal B, HER2-enriched, basal-like and claudin-low) [13,21,22]. Global gene expression profile analysis (Accession number GSE32905) classified tumors developed by WAP-Cre;*K-rasG12D*; *Twist1* transgenic mice as claudin-low (Figure S1). Immunostaining of epithelial and mesenchymal markers (Figure 2D) and quantitative RT-PCR analysis (lack of E-cadherin and claudin expression, high expression of vimentin; Figure S2) were highly consistent with this classification. Of note, endogenous expression of the *Zeb1*, *Zeb2* and *Twist2* EMT inducers was also induced (Figure S2), further supporting the

association of the EMT interactome with the claudin-low breast cancer subtype [23].

#### TWIST1 and ZEB1/2 transcription factors foster malignant transformation of human mammary epithelial cells and provide cells with a basal-like or a claudin-low signature, according to the extent of EMT

Both basal-like and claudin-low subgroups are aggressive, chemoresistant, triple-negative carcinomas (estrogen-receptor-, progesterone-receptor-, and HER2-negative). Yet claudin-low tumors exhibit several characteristic features, including low expression of adherens and tight junction proteins, a low level of luminal/epithelial differentiation, stem cell-like features, and a high frequency of metaplastic differentiation [24]. These tumors are believed to originate from an early epithelial precursor with inherent stemness properties and metaplastic features [24–26]. Nevertheless, the observation of claudin-low tumors in WAP-Cre;*K-RasG12D*; *Twist1* transgenic mice suggested that the development of these neoplasms could rely upon an EMT-driven

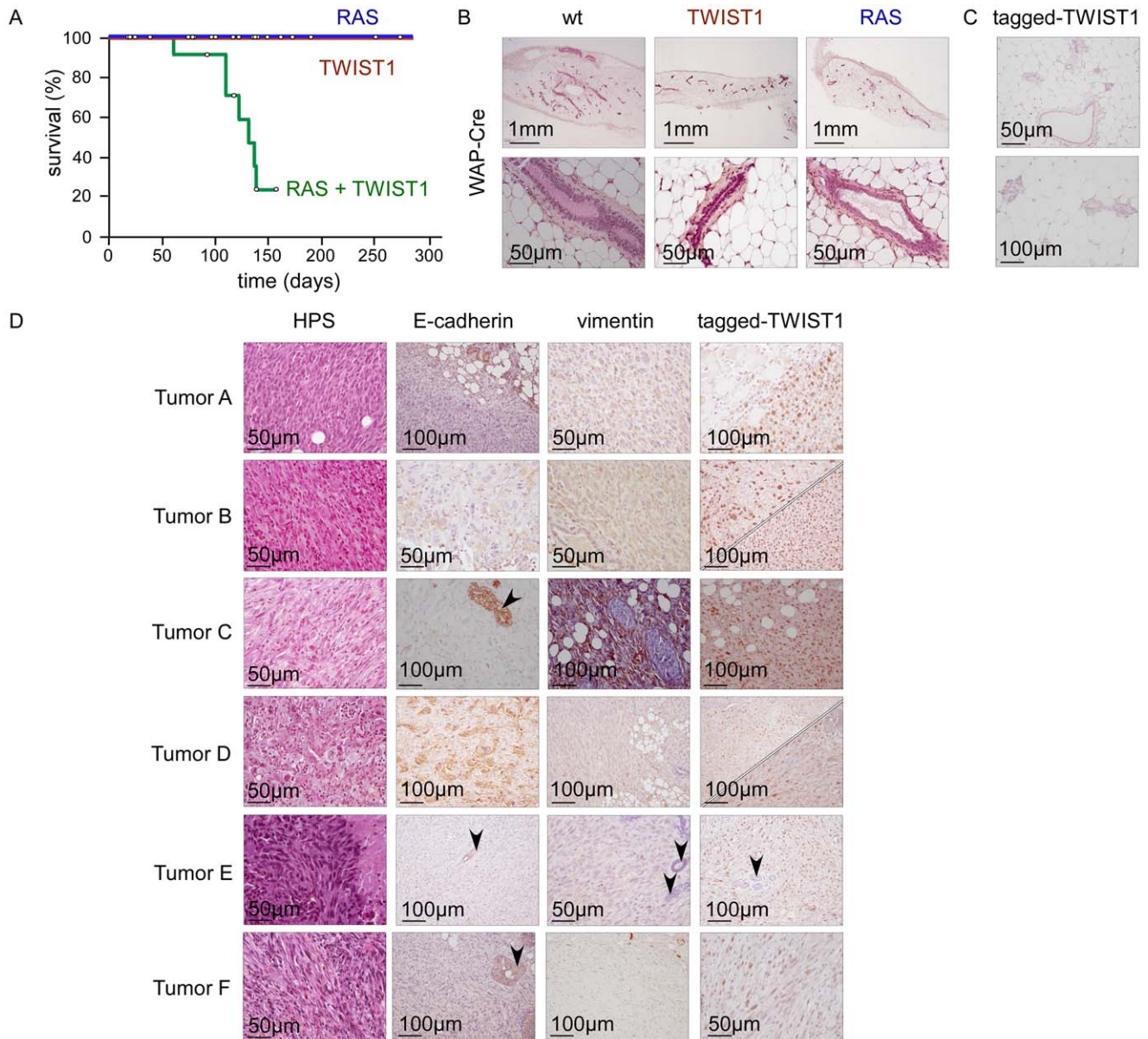


**Figure 2. *Twist1* promotes tumor initiation *in vivo*.** Transgene expression was driven by WAP-Cre. While WAP-Cre;*Twist1* (TWIST1; n = 25) and WAP-Cre;*K-RasG12D* (RAS; n = 19) mice remained healthy, WAP-Cre;*K-RasG12D*;*Twist1* females (RAS+TWIST1; n = 21) developed metaplastic mammary carcinomas. (A) Kaplan-Meier survival curves of transgenic mice. Survival corresponds to the end point of the experiment, the tumor burden requiring euthanasia of the animal. Open circles indicate mice censored from the dataset. (B) HPS staining of mammary glands from either wild-type (wt), *Twist1* or *K-rasG12D* transgenic mice. (C) Expression analysis of ectopic TWIST1 in mammary glands of nulliparous WAP-Cre;*Twist1* mice as assessed by IHC shows that the WAP promoter is active in a few epithelial cells. (D) Characterization of the WAP-Cre;*K-RasG12D*;*Twist1* mice-derived mammary carcinomas (RAS+TWIST1). RAS and TWIST coexpression leads to the development of metaplastic carcinomas characterized by a predominant E-cadherin<sup>-</sup>, vimentin<sup>+</sup> fusiform contingent (tumors A, C, E, F) or the presence of two epithelial-like (E-cadherin<sup>+</sup>) and fusiform (vimentin<sup>+</sup>) cell contingents (tumors B and D). For tumors B and D, both epithelial (upper panel) and fusiform (lower panel) cell contingents express the tagged-TWIST1 transgenic protein, demonstrating that fusiform cells originate from the epithelial ones. Normal epithelial cells are arrowed. doi:10.1371/journal.pgen.1002723.g002

process affecting epithelial cells formerly engaged in differentiation. We sought to test this hypothesis by mimicking in non-stem cells events occurring commonly in this breast cancer subtype. Claudin-low tumors and cell lines frequently exhibit increased levels of the EMT-inducing transcription factors TWIST1, ZEB1, and ZEB2 [13] and show activation of RAS/MAPK pathway components [24,27]. To functionally reproduce these two common features of claudin-low tumors, we performed oncogenic

cooperation assays by transducing genes encoding a single EMT inducer (TWIST1, ZEB1 or ZEB2) and/or an active form of H-RAS (H-RAS<sup>G12V</sup>) into immortalized human mammary epithelial cells (hTERT-HMECs, thereafter named HME cells). As in all experiments the infection efficiency exceeded 80%, the hypothesis of selection of a rare subpopulation of parental cells can be ruled out. Forced expression of an EMT inducer triggered acquisition of EMT features, including significant upregulation of mesenchymal

markers (i.e., vimentin, fibronectin) and decreased expression of genes involved in epithelial cell-cell adhesion (i.e., E-cadherin, occludin) (Figure 3). However, the degree of EMT commitment observed after infection was highly dependent on the EMT-inducing transcription factor, both in the absence or in the presence of the active form of RAS. In the absence of the mitogenic oncoprotein, ZEB1 expression was sufficient to promote a complete transdifferentiation process, giving rise to typical spindle-like cell morphology, and a total loss of E-cadherin expression (Figure 3; HME-ZEB1 cells). In contrast, ZEB2-expressing cells (HME-ZEB2 cells) and TWIST1-expressing cells (HME-TWIST1 cells) exhibited intermediate phenotypes, maintaining significant levels of E-cadherin expression and retaining a cobblestone morphology despite increased levels of mesenchymal markers such as vimentin and fibronectin (Figure 3). Transduction of an active form of RAS further promoted EMT induction, as assessed by cell morphology (Figure 3A) and protein expression analysis (Figure 3F and 3G). Nevertheless, HME-ZEB2-RAS and HME-TWIST1-RAS cells still exhibited an intermediate phenotype. Importantly, combining the mitogenic oncoprotein with either TWIST1, ZEB1 or ZEB2 was sufficient to provide cells with transformation potential, as assessed by their ability to form colonies in an assay on semi-solid medium and by acquisition of a characteristic stellate phenotype in 3D cell culture (Figure 3C and 3D). This observation suggested that EMT inducers could exert a potent oncogenic activity in the absence of a complete EMT. Global gene expression array analysis was next performed on freshly established cell lines (Accession number GSE32905). Strikingly, HME-ZEB1 cells and HME-ZEB1-RAS cells were defined as basal-B ( $P=2.7\times 10^{-20}$  and  $2.4\times 10^{-22}$  respectively), reminiscent of claudin-low tumors [13,21], HME-TWIST1, HME-TWIST1-RAS and HME-ZEB2 as basal-A ( $P=3.6\times 10^{-8}$ ,  $P=1.1\times 10^{-2}$ ,  $P=3.8\times 10^{-9}$  respectively), remi-

niscient of basal-like tumors [13,21], while HME-ZEB2-RAS positively correlated with basal-A/basal-like ( $P=5.0\times 10^{-2}$ ) and basal-B/claudin-low ( $P=2.3\times 10^{-2}$ ) (Figure 4 and Figure S3), suggesting a direct link between the extent of EMT and the intrinsic subtype. Confirming this hypothesis, exposure of HME-TWIST1-RAS and HME-ZEB2-RAS to the EMT-promoting cytokine TGF $\beta$  triggered a complete EMT with a shift to basal-B/claudin-low ( $P=2.3\times 10^{-18}$  for TGF $\beta$ -treated HME-TWIST1-RAS cells;  $P=6.8\times 10^{-22}$  for TGF $\beta$ -treated HME-ZEB2-RAS cells) (Figure 4 and Figure S3).

The extent of the EMT and the basal-B/claudin-low profiling were strongly associated with acquisition of stem cell-like features, as judged by the ability to form mammospheres under non-adherent culture conditions (Figure 3E) and by the fraction of cells exhibiting the CD44<sup>+</sup>/CD24<sup>-/low</sup> stem-like antigenic phenotype (respectively 84.5%, 83.2%, 20.6% and 15.3% of HME-ZEB1; HME-ZEB1-RAS, HME-ZEB2-RAS and HME-TWIST1-RAS; Figure 5). The gain of a mammary stem cell signature was also revealed by the use of the recently described Genomic Differentiation Predictor [13], following global gene expression array analysis on freshly established cell lines (Figure 6). Cells exhibiting the more pronounced mesenchymal phenotype (HME-ZEB1, HME-ZEB1-RAS; HME-ZEB2-RAS treated with TGF $\beta$  and HME-TWIST1-RAS treated with TGF $\beta$ ) exhibited a mammary stem like signature, whereas cells with an epithelial or an intermediate phenotype (HME, HME-TWIST1, HME-TWIST1-RAS; HME-ZEB2; HME-ZEB2-RAS) showed a luminal progenitor signature.

As expected from earlier studies [28–30], immortalized HMEC cells into which only H-RAS<sup>G12V</sup> had been transduced (HME-RAS) exhibited a low transformation potential (Figure 3D). Characterization of the few colonies growing on soft agar revealed a constant endogenous activation of EMT inducers, including

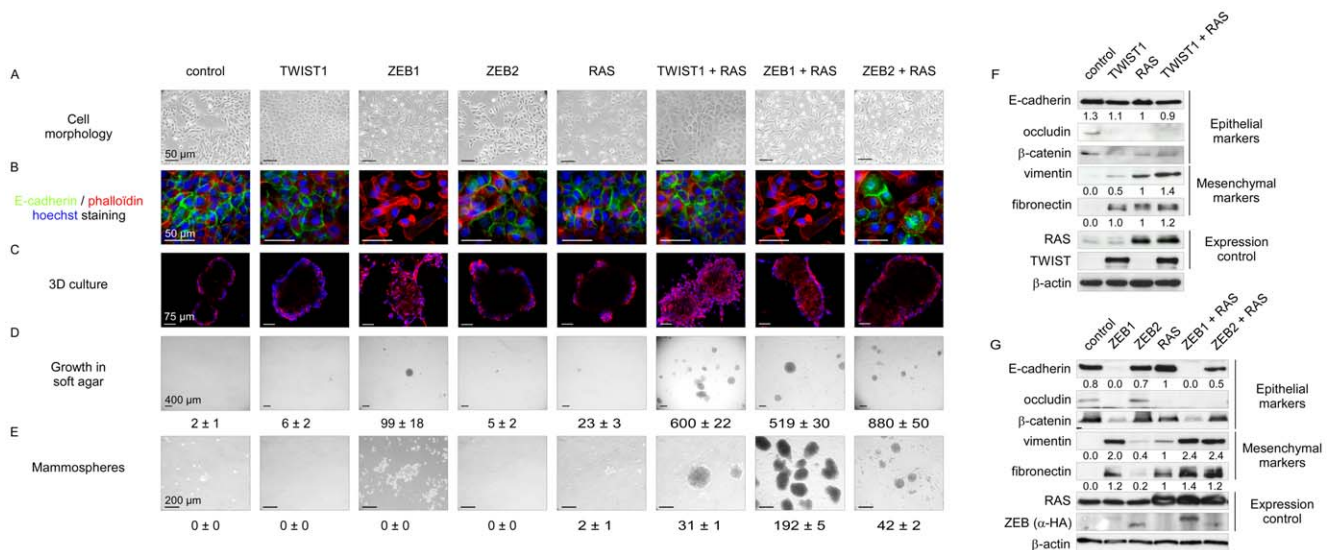


**Figure 3. EMT induction by embryonic transcription factors facilitates HMEC transformation by an activated form of RAS.** Sequentially, HMECs were immortalized with hTERT (control) and infected with retroviral expression constructs for TWIST1, ZEB1, or ZEB2 and H-RAS<sup>G12V</sup> (as depicted on top). (A) Representative photomicrographs of cells obtained by phase contrast microscopy. (B) E-cadherin expression analysis by immunofluorescence. (C) Cell morphology in 3D culture. (D) Transformation potential analysis by means of a soft agar colony formation assay. Numbers of colonies are indicated  $\pm$  SD of three replicates. (E) Mammosphere formation assay under low adherence conditions. Numbers of mammospheres per 20 000 cells are indicated  $\pm$  SD of three replicates. (F–G) Expression analysis of TWIST1, ZEB1, ZEB2, H-RAS, and of epithelial and mesenchymal markers by western blotting. Quantification of E-cadherin, vimentin and fibronectin signals, normalized with respect to  $\beta$ -actin expression and HMEC-hTERT-RAS derivatives is shown. doi:10.1371/journal.pgen.1002723.g003

## HMEC-hTERT-

A

Tumor subtype	Control	TWIST1	ZEB1	ZEB2	RAS	TWIST1 + RAS	ZEB1 + RAS	ZEB2 + RAS	TWIST1 + RAS + TGFβ	ZEB2 + RAS + TGFβ	shp53 RAS Epi.	shp53 RAS Mes.	MCF7	MDA-MB157
Basal-like Basal A	0.321 1.0E-08	0.309 3.6E-08	-0.145 1.1E-02	0.329 3.8E-09	0.256 5.8E-06	0.205 1.1E-02	-0.126 2.8E-02	0.130 5.0E-02	-0.236 3.1E-05	-0.249 1.1E-05	0.244 1.7E-05	-0.192 7.5E-04	-0.399 4.6E-13	-0.085 1.4E-01
Claudin-low Basal B	-0.185 1.2E-03	-0.479 6.1E-19	0.495 2.7E-20	-0.043 4.5E-01	-0.006 9.2E-01	-0.094 1.0E-01	0.518 2.4E-22	0.140 2.3E-02	0.472 2.3E-18	0.513 6.8E-22	-0.362 6.8E-11	0.438 9.4E-16	-0.718 <1E-35	0.224 7.7E-05
Luminal	-0.027 6.4E-01	0.143 1.2E-02	-0.084 1.5E-01	-0.138 1.6E-02	-0.168 3.2E-03	0.036 5.3E-01	-0.076 1.8E-01	-0.041 4.8E-01	-0.082 1.5E-01	-0.082 1.5E-01	0.037 5.2E-01	-0.081 1.6E-01	0.612 1.1E-32	-0.143 1.2E-02

B

ID	Gene symbol	Control	TWIST1	ZEB1	ZEB2	RAS	TWIST1 + RAS	ZEB1 + RAS	ZEB2 + RAS	TWIST1 + RAS + TGFβ	ZEB2 + RAS + TGFβ	shp53 RAS Epi.	shp53 RAS Mes.	MCF7	MDA-MB157
209173_at	<i>AGR2</i>	439.1	1769.9	32.4	314.6	763.4	791.8	69.7	176.3	149.9	213.6	655.9	61.7	5174.0	31.5
201131_s_at	<i>CDH1</i>	4867.6	4980.9	77.7	4069.4	3895.4	5341.3	105.8	2976.0	441.2	56.0	5594.5	126.0	9390.2	38.4
101428_at	<i>CLDN4</i>	375.8	340.3	72.8	132.6	233.1	327.0	48.2	233.2	92.8	90.3	1607.3	111.6	950.4	78.8
202790_at	<i>CLDN7</i>	362.4	1246.4	120.9	381.1	463.0	405.9	155.1	241.0	135.1	145.5	2101.0	119.6	902.5	96.7
201839_at	<i>EpCAM</i>	4498.9	2925.6	60.9	3691.7	6118.1	5121.3	35.2	1986.5	387.0	93.9	4969.1	31.4	10277.9	309.9
209008_at	<i>KTR8</i>	2140.6	2424.5	1280.9	1885.0	2597.0	1084.5	509.1	728.1	824.2	703.7	2845.9	626.9	7243.1	592.7
201596_at	<i>KTR18</i>	8310.8	4198.9	2412.3	7678.0	11135.9	7832.3	1771.6	4992.5	3722.2	3233.3	7524.1	1102.1	20334.6	6818.5
227492_at	<i>OCLN</i>	745.4	1047.5	28.3	474.0	547.0	657.5	36.8	265.7	49.6	47.6	1580.0	44.6	2068.8	254.2
231022_at	<i>OCLN</i>	168.4	273.5	36.2	138.7	148.5	130.6	56.1	107.3	42.2	55.7	257.5	69.2	452.8	89.3
213139_at	<i>SNAI2</i>	2628.2	2796.2	5335.8	3159.1	3202.0	3326.7	6865.7	4736.4	5594.4	6423.6	2181.9	6104.9	40.3	5141.3
201666_at	<i>TIMP1</i>	1576.4	1734.5	6540.6	2803.7	2989.9	2471.2	6893.8	5680.2	2180.6	3903.8	4050.4	17369.6	918.1	5353.5
213943_at	<i>TWIST1</i>	468.8	397.9	1734.6	514.0	508.1	536.5	1493.6	1210.2	754.5	879.6	258.5	4282.4	27.7	2575.9
229404_at	<i>TWIST2</i>	376.9	271.1	610.6	486.5	539.8	417.2	476.03	418.3	773.0	849.2	202.6	1069.8	18.4	546.8
201426_at	<i>VIM</i>	4982.2	1099.9	13962.7	5295.2	5449.5	4431.8	12679.0	9650.1	16355.4	15528.4	6183.4	17812.6	79.9	20693.0
212758_s_at	<i>ZEB1</i>	32.5	31.4	235.6	25.8	31.1	46.0	146.7	63.0	331.1	203.0	30.9	299.1	27.8	116.3
272764_at	<i>ZEB1</i>	13.8	10.5	452.1	19.0	14.4	73.9	533.2	159.3	1425.3	1242.8	17.9	2197.9	8.4	485.0
203603_at	<i>ZEB2</i>	9.0	41.6	206.9	10.9	5.8	68.7	655.9	225.3	227.1	226.5	5.8	317.0	11.0	358.2
228333_at	<i>ZEB2</i>	9.63	32.79	80.9	13.4	9.28	19.35	165.7	96.4	80.0	89.5	7.9	113.3	8.0	89.6
203729_at	<i>EMP3</i>	143.4	73.1	654.4	122.9	177.5	149.0	329.3	134.6	571.7	496.5	189.1	1118.4	38.5	255.9
208782_at	<i>FSTL1</i>	1325.2	972.5	2866.0	1590.3	1688.4	1461.7	3769.1	1863.2	3966.7	3608.1	494.7	3696.6	23.9	5090.0
214085_x_at	<i>GLIPR1</i>	948.7	321.0	2332.8	811.4	764.6	1118.1	982.3	809.4	2932.7	2351.1	195.9	1433.1	210.2	1146.5
213262_at	<i>SACS</i>	406.8	172.1	958.6	436.9	531.1	512.5	1015.7	713.9	2734.2	2531.1	177.8	949.9	177.2	731.2
209651_at	<i>TGFβ111</i>	778.1	900.7	1463.5	1008.4	742.1	722.8	2035.1	1371.2	1885.6	1882.6	1053.8	2818.4	11.0	1642.8
212190_at	<i>SERPINE2</i>	2679.1	524.0	7278.1	2707.4	2703.6	3860.0	9465.7	5506.1	9379.4	12088.5	1590.7	12414.5	62.5	2581.7
204115_at	<i>GNG11</i>	306.2	67.4	1369.9	197.2	237.4	483.1	2036.3	490.2	2100.5	2290.2	26.9	2422.1	13.0	1515.8
204620_s_at	<i>VCAN</i>	484.4	150.5	1667.0	945.5	605.5	1789.9	2273.6	2069.1	8051.2	8795.9	60.6	5228.1	22.1	2488.6
221731_x_at	<i>VCAN</i>	713.2	222.3	2486.0	1351.3	861.0	2641.1	3606.2	3186.5	11959.1	12878.3	90.9	6904.5	21.3	3694.7
202766_s_at	<i>FBN1</i>	57.6	32.3	3013.9	127.4	51.4	367.3	1049.4	395.4	3669.9	3463.6	52.0	7097.6	60.8	1387.5
213325_at	<i>PVRL3</i>	167.2	52.7	419.1	68.5	96.0	198.1	325.1	211.3	610.0	507.9	35.8	546.1	83.3	1497.2
213338_at	<i>TMEM158</i>	208.6	111.6	750.7	273.2	300.5	343.6	546.8	358.3	1385.0	1255.2	87.0	2572.5	33.7	240.3
204733_at	<i>KLK6</i>	230.7	256.3	69.7	169.0	293.4	112.2	42.5	72.6	53.9	52.9	275.7	62.5	180.8	34.4
206125_s_at	<i>KLK8</i>	668.6	2276.9	48.1	590.0	695.7	470.2	65.9	287.0	76.5	50.7	3369.7	95.9	123.5	60.0
202525_at		142.4	294.4	37.2	157.3	154.7	86.3	36.2	63.7	46.8	41.2	971.0	67.1	475.1	34.3
210827_s_at	<i>ELF3</i>	594.5	2123.5	36.8	578.7	398.0	658.7	90.1	396.9	33.3	27.8	1027.6	38.0	757.9	47.0
218186_at	<i>RAB25</i>	776.6	1852.8	26.4	706.4	844.6	487.2	29.6	354.9	30.3	26.2	2120.2	44.0	1702.7	23.0
204667_at	<i>FOXA1</i>	404.7	287.2	45.3	236.4	163.7	429.2	44.5	415.8	49.4	63.2	278.5	27.5	1353.3	22.5

**Figure 4. Mesenchymal HMEC-derivatives display a claudin-low gene expression signature.** (A) Statistical values of the Pearson's correlation to the centroids of intrinsic gene clusters determined according to the cell line gene expression data set of Neve and collaborators [21]. (B) The expression of significant genes from the claudin-low signature [13,21] is shown. Relative transcript abundance with highest expression is labeled in red and with lowest expression is labeled in green, respectively. MCF7 and MDA-MB157 were used as internal luminal and claudin-low controls, respectively.

doi:10.1371/journal.pgen.1002723.g004

*TWIST1*, *ZEB1* and *ZEB2* (Figure S4), and a mesenchymal phenotype, further highlighting the deleterious interplay between the mitogenic oncoprotein and EMT-promoting factors. To

confirm the association between the RAS-induced transformation and the endogenous expression of EMT inducers, immortalized HMECs were transduced with an H-RAS<sup>G12V</sup> and sorted by flow

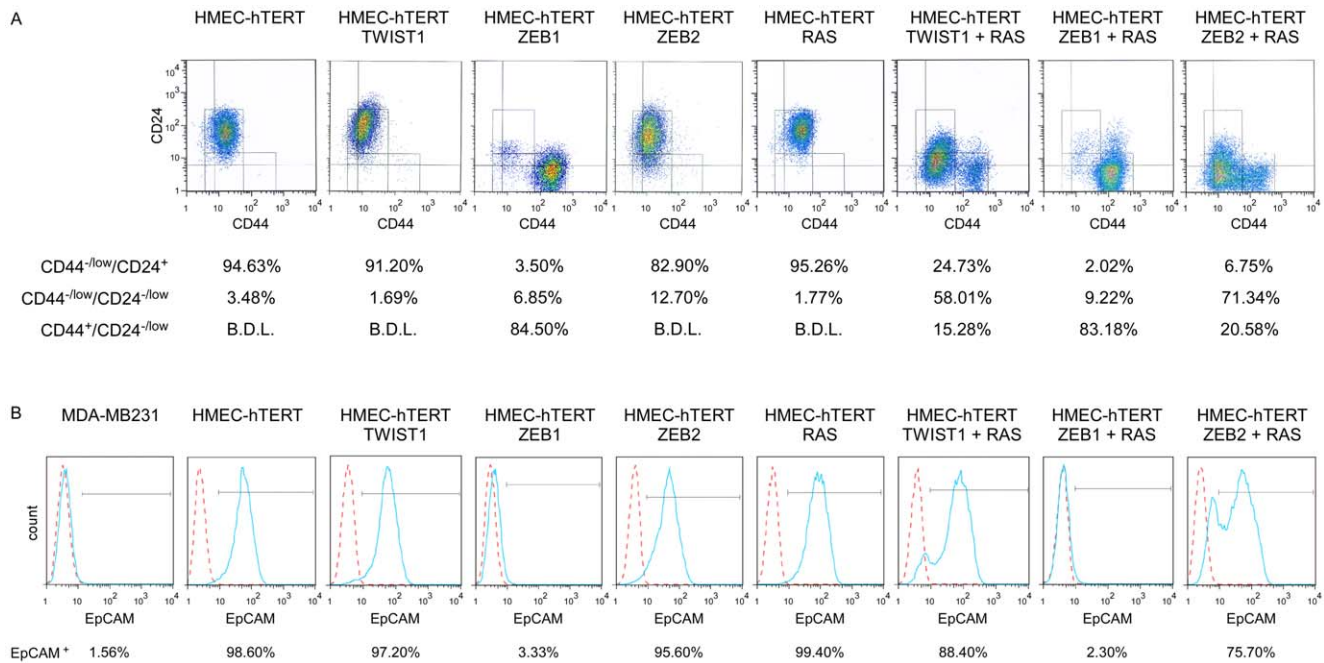


**Figure 5. Combined expression of H-RAS<sup>G12V</sup> and EMT-inducing transcription factors provides HMEC cells with a stem cell-like antigenic phenotype.** Analysis by flow cytometry of the expression of CD44, CD24 (A) and EpCAM (B). Solid blue lines represent staining with FITC-anti-EpCAM antibody and dotted red lines represent staining with FITC-conjugated isotype control. B.D.L.: Below Detection Limit. The claudin-low mesenchymal breast cancer cell line MDA-MB231 was used as a negative EpCAM staining control. doi:10.1371/journal.pgen.1002723.g005

cytometry using the EpCAM epithelial antigen. EpCAM-positive epithelial cells were next cultured in the presence of TGF $\beta$ . As shown in Figure S5, TGF $\beta$  exposure triggered morphological and phenotypical features of EMT, associated with increased expression of *TWIST1*, *TWIST2*, *ZEB1* and *ZEB2* EMT inducers.

Reactivation of these transcription factors was associated with the acquisition of a transformed phenotype.

Taken together, these observations showed that activation of EMT inducers, through either forced expression or endogenous induction, fosters malignant transformation of mammary epithelial

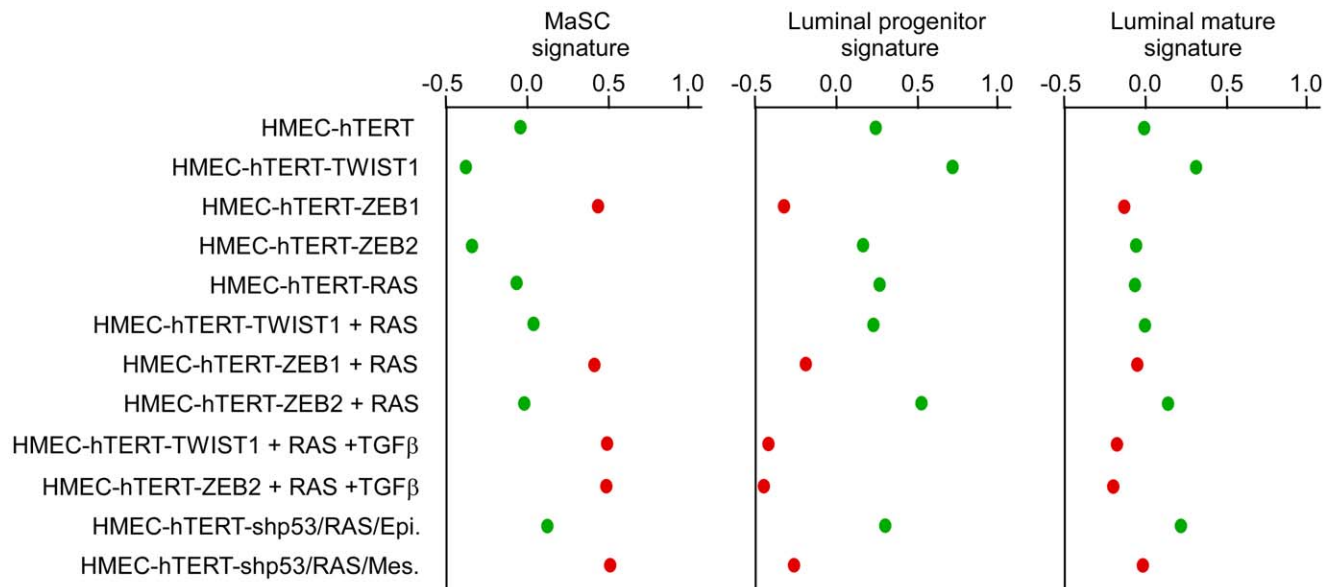


**Figure 6. Expression of EMT-inducing transcription factors triggers a dedifferentiation of HMEC cells.** Mammary stem cells (MaSC), luminal progenitor and luminal mature signatures of human cell line are defined according to Lim and collaborators [25], respectively. High scores are indicative of a good correlation between the analyzed gene expression profiles and the established signatures. Cells lines with an epithelial morphology are labeled in green while cell lines harboring a mesenchymal morphology are labeled in red. doi:10.1371/journal.pgen.1002723.g006

cells and confers to them basal-like or claudin-low signatures, according to the extent of transdifferentiation.

### EMT commitment triggers malignant transformation of human mammary epithelial cells deficient for p53- and RB-dependent pathways

Our data demonstrated that EMT inducers can promote transformation of mammary epithelial cells. We and others have previously shown that the TWIST and ZEB proteins can functionally inhibit p53- and RB-dependent pathways, preventing cells from undergoing oncogene-induced senescence and apoptosis [10–12]. To test whether the oncogenic properties of EMT-inducing transcription factors act only to lift these two oncosuppressive barriers or whether they might be involved in additional processes, we have generated human mammary epithelial cells deficient in both pathways. The *INK4A* tumor suppressor, a crucial regulator of the RB-dependent pathway, is known to be silenced by progressive promoter methylation in HMECs escaping from stasis [31]. We depleted these cells of p53 by means of RNA interference (using a shRNA *TP53* thereafter named shp53 or, as a control, a scrambled shRNA). Knockdown of p53 was checked by western blotting and by demonstrating that, in response to DNA damage, p53 induction and the resulting G1 growth arrest were abolished (Figure S6). Cells were next infected with H-RAS<sup>G12V</sup> and immortalized by transfection with hTERT to generate shp53/H-RAS<sup>G12V</sup>/hTERT HMECs (hereafter named HME-shp53-RAS cells). Characterization of the colonies generated after growth of these cells in soft agar demonstrated that a vast majority of them expressed mesenchymal markers (Figure S7E). This observation led us to hypothesize that a subset of HME-shp53-RAS cells committed spontaneously to an EMT program and that initiation of the transdifferentiation process promoted cell transformation. In support of the first hypothesis, cells exhibiting a cobblestone phenotype and expressing epithelial markers (E-cadherin<sup>+</sup> and EpCAM<sup>+</sup>) and cells displaying a fibroblastic morphology and exhibiting mesenchymal markers (vimentin<sup>+</sup>) were found to coexist in HME-shp53-RAS cells (Figure S7C). Epithelial and mesenchymal cell subpopulations were next sorted on the basis of their differential antigenic phenotypes (EpCAM<sup>+</sup> and EpCAM<sup>-</sup> respectively) (Figure S8). The phenotypes of the epithelial and mesenchymal cell populations were confirmed by assessing the expression of additional epithelial markers ( $\beta$ -catenin, E-cadherin, ZO-1, and occludin) and mesenchymal markers (fibronectin and vimentin) by immunofluorescence staining and western blotting (Figure S9). The sorted mesenchymal-cell subpopulations specifically displayed EMT-associated features such as motility, invasiveness, and a stellate phenotype when cultured in 3D (Figure 7). Gene profile analysis classified these mesenchymal cells as claudin-low/basal B, while epithelial HME-shp53-RAS cells were classified as basal-like/basal A (Figure 4 and Figure S3). Although epithelial and mesenchymal HMEC derivatives exhibited similar H-RAS<sup>G12V</sup> expression levels (Figure S10), only mesenchymal cells grew in soft agar and gave rise to tumor formation, within three months, when homotopically xenografted in *nude* mice (6 of 7 mice, Figure 7).

These observations demonstrated that EMT commitment fosters malignant transformation of human mammary epithelial cells deprived of functional p53- and RB-dependent pathways. To further confirm this hypothesis sorted epithelial HME-shp53-RAS cells were treated with TGF $\beta$ . Exposure to this EMT-inducing cytokine triggered a pronounced shift from epithelial to mesenchymal markers, associated with induction of *ZEB1* (200-fold) and *ZEB2* (10-fold) (data not shown) and with a dramatic gain in anchorage-independent growth properties (Figure S11). Importantly,

forced expression of ZEB1 in sorted epithelial HME-shp53-RAS cells was sufficient to mimic TGF $\beta$  exposure, promoting both EMT and cell transformation (Figure S12).

### TWIST1 and ZEB1/2 transcription factors downregulate the oncosuppressive PP2A activity

Our observations strongly suggested that, beyond the inhibition of the p53- and RB-dependent pathways, EMT inducers display additional, as yet unidentified oncogenic activities. It has been previously shown that, *in vitro*, transformation of normal human epithelial cells, including mammary epithelial cells, requires disruption of the telomere maintenance system and dysregulation of at least four key signaling pathways: activation of the RAS-dependent pathway and inhibition of the p53-, RB-, and protein phosphatase 2A-dependent pathways [28–30]. We thus endeavored to analyze the effects of EMT commitment on protein phosphatase 2A (PP2A) activity. PP2A is a ubiquitously expressed serine/threonine phosphatase accounting, with protein phosphatase 1 (PP1), for 90% of all the serine/threonine phosphatase activity in the cell [32]. By using a peptide substrate (synthetic phosphothreonine peptide RRA(pT)VA) compatible with the phosphatase activity of PP2A but not with that of PP1 and by employing experimental conditions ensuring the specificity of PP2A activity (see Materials and Methods), we found sorted mesenchymal HME-shp53-RAS cells to exhibit lower phosphatase activity than sorted epithelial HME-shp53-RAS cells (Figure 8). More importantly, expression of either TWIST1, ZEB1, or ZEB2 in HME cells was sufficient to trigger significant (2-fold) downregulation of serine/threonine phosphatase activity, revealing a novel oncogenic feature of these proteins. This downregulation was similar to that observed in immortalized HMECs transformed with H-RAS<sup>V12</sup> and the SV40 large T and small t antigens (HMLER cells; Figure 8), the small t antigen being known to inhibit PP2A activity [33]. Notably, claudin-low HME-ZEB1-RAS cells exhibited 4-fold lower phosphatase activity than immortalized HMECs (Figure 8).

### Discussion

Whereas TWIST1 has been convincingly implicated in the metastatic dissemination of breast cancer cells, these data underscore the importance of EMT-inducing transcription factors in driving mammary carcinogenesis, with a dual role in cell transformation and dedifferentiation. Tumor development has been portrayed as a multistep processes with a progressive acquisition of genetic and epigenetic abnormalities providing cells with biological capabilities such as sustained proliferation, replicative immortality, survival advantages, angiogenesis and, in some cases, invasive growth and metastasis [34]. According to the Darwinian model of cancer development, each of these acquired traits confers a distinct selective advantage, originating successive waves of clonal expansion that drive tumor progression. It is well known that this complex and time consuming process requires abrogation of several oncosuppressive barriers. In epithelial cells, including mammary epithelial cells, these barriers comprise the p53-, RB- and PP2A-dependent pathways [28–30]. We and others have previously demonstrated that TWIST and ZEB transcription factors were capable to inhibit p53- and RB- dependent pathways [10–12]. Remarkably, our observations reveal that activation of these factors in HMECs also affects PP2A phosphatase activity. Considerable evidence highlights the tumor-suppressor functions of this serine/threonine phosphatase. For example, it has been shown *in vitro* that the transforming ability of the SV40 small t antigen requires interactions with PP2A and downregula-



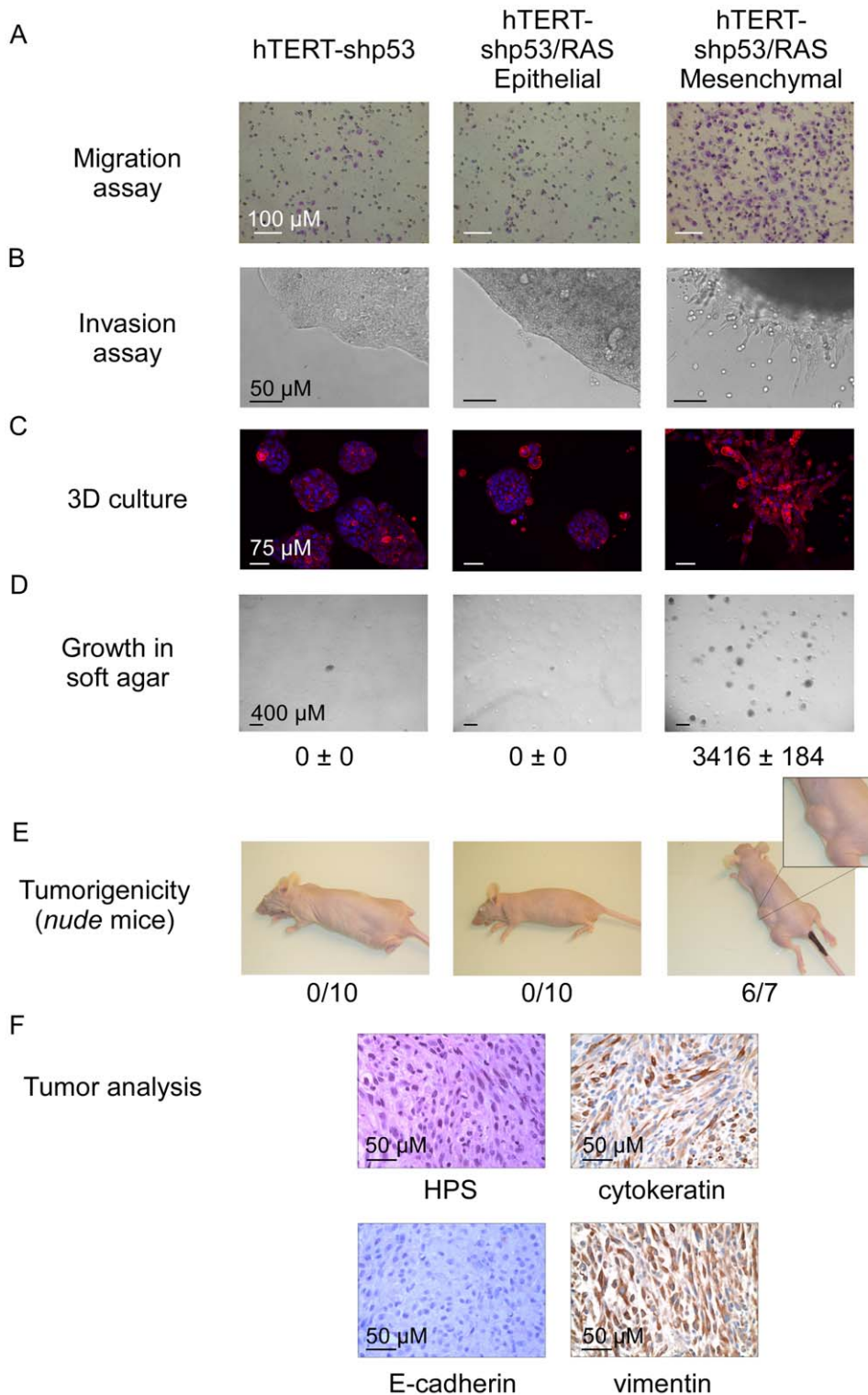


**Figure 7. Characterization of epithelial and mesenchymal hTERT-shp53/RAS HMEC-derivative subpopulations.** (A, B) Migratory and invasive properties analyses as assessed by Boyden chamber migration and Matrigel invasion assays, respectively. (C) Cellular morphology in 3D culture. (D) Transformation potential analysis assessed by a soft agar colony formation assay. Numbers of colonies are indicated  $\pm$  SD of triplicate counting. (E) Tumorigenic potential analysis assessed by homotopically xenografts in *nude* mice. Numbers of mice developing tumors are indicated. (F) Tumor histology: Hematoxylin-Phloxin Saffranin staining (HPS) and cytokeratin, E-cadherin and vimentin expression analysis assessed by immunohistochemistry.

doi:10.1371/journal.pgen.1002723.g007

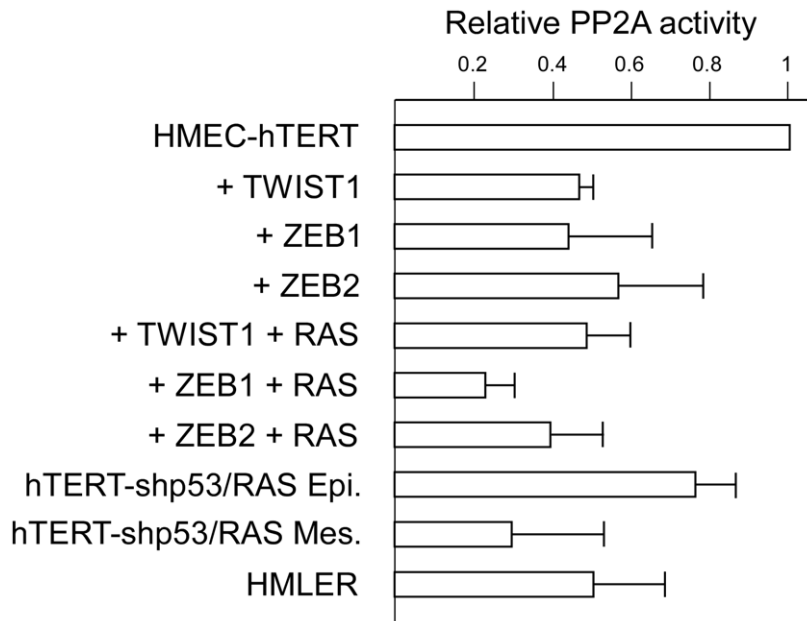


**Figure 8. Assessment of PP2A activity in hTERT-HMEC derivatives.** PP2A phosphatase activity was assessed and normalized with respect to the parental hTERT-HMEC cells. Activities are expressed in arbitrary units  $\pm$  SD of triplicate experiments. hTERT-HMECs transduced with SV40 T/t antigens and H-RAS<sup>G12V</sup> (HMLER, [29]) were used as an internal positive control. doi:10.1371/journal.pgen.1002723.g008

tion of its activity [34–36]. *In vivo*, mutations affecting different components of the PP2A holoenzyme complex have been identified in a variety of human malignancies and, in mouse models, mutation of PP2A favors tumorigenesis [37]. Loss of PP2A during cell transformation triggers multiple events, such as upregulation of kinases involved in mitogenic and survival signaling (e.g. AKT and MAPK), stabilization of protooncogenes (e.g. *MYC*), destabilization of tumor suppressors (e.g. p53 and RB), and loss of proapoptotic signaling pathways (e.g. BAD) [32]. Modulation of downstream components of the RAS signaling pathway by PP2A might be of particular significance in our model, as the ability of PP2A to antagonize the oncogenic properties of RAS by dephosphorylating crucial downstream effectors such as c-MYC and AKT makes its downregulation a prerequisite to RAS-induced malignant transformation. The modulation of PP2A activity by EMT inducers might thus be an important mechanism underlying the deleterious cooperation of these factors with oncogenic RAS in cell transformation. The inhibition of PP2A activity by EMT inducers might also be relevant during embryogenesis, as PP2A appears as a negative regulator of the WNT signaling cascade [38] which is required for several crucial steps in early development. Further studies are needed, however, to better characterize the mechanisms involved in this regulatory process, as PP2A represents a complex family of holoenzyme complexes known to display different activities and to exhibit diverse substrate specificities [39].

Given the importance of p53-, RB- and PP2A-dependent protective barriers against tumorigenesis and their role in regulating cell differentiation and self-renewal [40], aberrant reactivation of EMT inducers might profoundly affect the multistep nature of tumorigenesis by increasing cell plasticity and leapfrogging the mutation bottleneck toward tumor progression. This view is supported by our *in vitro* transformation assays demonstrating that, upon a single mitogenic activation, forced expression of either TWIST1 or ZEB1/2 is sufficient to trigger malignant conversion of immortalized human mammary epithelial

cells (hTERT-HMECs). It is also consistent with the observed rapid and repeated appearance of multifocal breast carcinomas in WAP-Cre;*K-rasG12D*;*Twist1* mice. It is further supported by the work by Phuoc T. Tran and colleagues, who demonstrated in an elegant inducible transgenic mouse model that TWIST1 overexpression accelerates K-RAS-induced lung tumorigenesis [41]. Several phenomena associated with tumor initiation, such as inflammation [42], physical constraints (including hydrostatic pressure, shear stress and tension forces) [43], abnormal activation of signaling pathways such as those controlled by WNT, NOTCH, or TGF $\beta$  [4,44], and hyperactivation or RAS-ERK1/2 signaling [45] are known to trigger expression of EMT-promoting factors and could thus induce reactivation of these embryonic transcription factors in early stages of tumor development, as previously observed in animal models [46]. Moreover, beyond the deleterious consequences of aberrant reactivation of EMT inducers in differentiated or committed epithelial cells, the ability of EMT inducers to inhibit key oncosuppressive pathways also implies that embryonic or adult stem cells that normally express these factors are particularly vulnerable to cell transformation.

Cooperation assays demonstrate that activation of EMT-inducing transcription factors such as TWIST1 or ZEB2 is sufficient to make cells highly prone to transformation, even in the absence of a complete mesenchymal morphological shift. In line with this view, immunohistochemical analysis of TWIST1 in human non-invasive breast cancers (ductal carcinomas *in situ*, DCIS) has revealed frequent overexpression of this EMT inducer within the bulk of the primary lesion, while the cancer cells maintain an epithelial phenotype (Figure S13). EMT is known to be a highly dynamic process giving rise to a series of important changes in cell phenotype, including loss of cell polarity, loss of cell-cell adhesion structures, remodeling of the cytoskeleton, and promotion of cell motility. As recently highlighted by Klymkowsky and Savagner, although the term EMT is generally applied as if it were a single conserved process, EMT-related processes can in fact vary in degree from a transient loss of cell polarity to total

reprogramming of the cell [47]. The existence of malignant cells with combined epithelial and mesenchymal characteristics has previously been demonstrated *in vivo*, in both mouse models of EMT and human tumors [48,49]. Especially, epithelial cells coexpressing cytokeratins 5/19 and vimentin have been identified by dual immunofluorescence labeling in claudin-low and basal-like breast cancers, two breast cancer subtypes frequently exhibiting overexpression of EMT-inducing transcription factors [13]. Overall, these observations strongly suggest that EMT-promoting factors can exert oncogenic functions in cells retaining an epithelial phenotype, in the total absence of morphological features of EMT, and probably long before initiation of the invasion-metastasis cascade.

Previous *in vitro* studies using human mammary epithelial cells have revealed a link between EMT, malignant transformation, and acquisition of stem cell properties. For example, the transformation of HMECs by means of a combination of hTERT, SV40 large T and small t antigens, and H-RAS<sup>G12V</sup> (HMLER cells) is associated with both mesenchymal and stem-like features [7,8,50]. In the absence of oncogenic RAS, introduction of SV40 T and small t antigens and hTERT into mammosphere-derived HMECs also generates malignant cells exhibiting EMT and stem-like properties [51]. Recent reports further demonstrate in human cancer cell lines that spontaneous EMT or TGF $\beta$ /TNF $\alpha$ -mediated EMT generates cells with a claudin-low phenotype [52,53]. Yet the intrinsic role of EMT inducers was not addressed in these studies. We highlight herein a dual role of these factors in cell transformation and dedifferentiation. Remarkably, in the context of a very few genetic events, the aberrant activation of an EMT inducer can initiate mammary epithelial cell transformation *in vitro* and *in vivo* and can drive the growth of undifferentiated tumors exhibiting all the characteristic features of claudin-low tumors, including a malignant phenotype, low expression of tight and adherens junction genes, EMT traits, and stem-cell-like characteristics.

The origin of the different intrinsic subtypes of human breast cancer is a topic of contentious debate and remains ill defined. Recent *in vitro* observations support the view that both luminal and basal-like breast cancers derive from a common luminal progenitor cell, whereas claudin-low tumors, viewed as the most primitive malignancies, originate from a stem/progenitor cell with inherent stemness properties and metaplastic features [24–26]. Others suggest that basal-like and claudin-low tumors arise from transformation of a similar stem cell, but that the claudin-low tumors stay arrested in an undifferentiated state, while basal-like cancer cells divide asymmetrically and give off differentiated progeny arresting at the luminal progenitor state [54]. Our observations pave the way for an alternative model highlighting a dynamic process orchestrated by the activity of EMT-inducing transcription factors. According to this model, aberrant activation of EMT inducers in committed cells (e.g. luminal progenitors) might foster initiation of triple-negative breast tumors and confer basal-like or claudin-low signatures, according to the extent of transdifferentiation. Our model also implies that basal-like tumors might progressively evolve towards a claudin-low phenotype through completion of the EMT process. This view is supported by the histopathology of human metaplastic breast tumors: phenotypically, the acquisition of mesenchymal features can occur at various stages of the disease [55], highlighting the dynamic role of transdifferentiation during tumor development and pointing to the interaction between cancer cells and the microenvironment as a key determinant of tumor phenotype and behavior. It is noteworthy that a model of murine claudin-low tumors has recently been described, involving transplantation of p53-null

mammary tissues into the cleared fat pads of wild-type recipients [56]. This observation is consistent with the role of p53 loss in EMT induction [57–59] and with the spontaneous generation of mesenchymal cells exhibiting a claudin-low phenotype in HME-shp53-RAS cells. Yet in this model described by Herschkowitz and colleagues, p53-null mouse mammary tumors fell into a variety of molecular groups, also including luminal and basal-like subtypes [56]. WAP-Cre;*K-rasG12D*;*Twist1* mice thus appear as the first mouse model consistently generating claudin-low tumors. These transgenic mice might thus serve as valuable preclinical models for testing both potential therapeutic agents targeting these aggressive neoplasms and potential preventive agents.

## Materials and Methods

### Constructs and mouse strains

The TWIST1-E12 tethered heterodimer was generated by PCR by fusing the human TWIST1 and E12 proteins using a G<sub>3</sub>-S<sub>2</sub>-G<sub>2</sub>-S-G<sub>3</sub>-S-G<sub>3</sub>-S<sub>2</sub>-G<sub>2</sub>-S-G<sub>3</sub>-S-G polylinker as described in [60]. The full-length murine HA-tagged ZEB1 and ZEB2 cDNAs were cloned into the pBabe retroviral construct. The *TP53* shRNA (shp53) pRETRO SUPER expression construct has been described in [61].

Animal maintenance and experiments were performed in a specific pathogen free animal facility “AniCan” at the CRCL, Lyon, France in accordance with the animal care guidelines of the European Union and French laws and were validated by the local Animal Ethic Evaluation Committee. The heterozygous knock-in LSL-*K-rasG12D* mouse strain [16] was crossed with CAG-LSL-*(Myc)-Twist1* mice (FVB background) [14]. Both TWIST1 monomer and T1-E12 dimers were used producing similar results [60]. *K-rasG12D*;*Twist1* offspring were subsequently crossed with mice carrying the Cre recombinase under the control of the Mouse Mammary Tumor Virus or Whey Acidic Protein promoters (MMTV-Cre (B6129F1 background) or WAP-Cre (c57BL/6 background) [17]; purchased from the NCI-MMHCC. Cre (wild type), Cre;*K-rasG12D*, Cre;*Twist1*, and Cre;*K-rasG12D*;*Twist1* virgin animals were maintained and monitored at least weekly for tumor incidence. End points were determined based on tumor diameter (>17 mm) or the sick appearance of an animal. Tissues were harvested and either snap frozen in N<sub>2</sub>(0) or immersed in formalin until pathological analysis. Genotyping of genomic DNA from tails purified using the NucleoSpin Tissue kit (Macherey-Nagel) was performed with primers described in references [14,16,17] using REDTaq 2 × ReadyMix (Sigma).

### Cell culture

Primary human mammary epithelial cells (HMECs) were provided by Lonza. HMEC-derivatives were cultured in 1:1 Dulbecco’s Modified Eagle’s Medium (DMEM)/HAMF12 medium (Invitrogen) complemented with 10% FBS (Cambrex), 100 U/ml penicillin-streptomycin (Invitrogen), 2 mM L glutamine (Invitrogen), 10 ng/ml human epidermal growth factor (EGF) (PromoCell), 0.5  $\mu$ g/ml hydrocortisone (Sigma) and 10  $\mu$ g/ml insulin (Actrapid).

Three-dimensional cultures consisted in culturing  $5 \times 10^3$  cells/well in 2% growth factor reduced Matrigel (BD Biosciences) on top of a 100% matrigel layer. 20 days after seeding, cells were fixed in 3% paraformaldehyde (Sigma), permeabilized in 0.5% Triton 100X (Sigma) in PBS buffer for 10 min. After several washes in PBS, cells were labeled with 1  $\mu$ g/ml of TRITC-conjugated Phalloidin P1951 (Sigma) for 45 min. Following washes in PBS, nuclei were stained with Hoechst 5  $\mu$ g/ml for 10 min and mounted with Fluoromount-G (SouthernBiotech).

For mammosphere formation, after filtration through a 30  $\mu\text{m}$  pore filter, single-cells were plated at a density of  $10^5$  cells/ml in Corning 3261 ultra-low attachment culture dishes. Primary cell spheres were enzymatically dissociated with 0.05% trypsin for 15 min at 37°C to obtain single-cell suspension. The ability to generate mammospheres was defined after three consecutive passages.

Treatment with TGF $\beta$  was performed with 2.5 ng/ml of the recombinant cytokine (Peprotech) for a three week period.

Cell distribution was performed using the FITC-EpCAM VU-1D9 (Stem Cell), the FITC-CD44 G44-26 (BD Pharmingen) and the PE-CD24 ML5 (BD Pharmingen) monoclonal antibodies, the FACScan Calibur (Becton Dickinson) and analyzed using the FlowJo software.

### Matrigel invasion assays

Matrigel (BD Biosciences) was added to the wells of an eight-well Labtek chamber in a volume of 300  $\mu\text{l}$ /well. A Matrigel plug of about 1 mm diameter was removed. The hole was successively filled with  $10^5$  cells and 100  $\mu\text{l}$  of Matrigel. Appropriate growth medium was added on top. Cultures were analyzed after 24 h (Figure 7) or 72 h (Figure S11). Areas of migration were visualized using an Olympus IX50 (NA 0.075). Samples were performed in duplicate.

### Transwell migration assay

$5 \times 10^4$  cells were placed in the upper chamber of an 8  $\mu\text{M}$  Transwells (BD Biosciences). 24 h later, chambers were washed twice with PBS. The filter side of the upper chamber was cleaned with a cotton swab. The membrane was next cut out of the insert. Cells were fixed in methanol and stained with 5% Giemsa 30 min at room temperature.

### Retroviral infection

$2 \times 10^6$  Phoenix cells were transfected by calcium-phosphate precipitation with 10  $\mu\text{g}$  of retroviral expression vectors. 48 h post-transfection, the supernatant was collected, filtered, supplemented with 5  $\mu\text{g}/\text{ml}$  of polybrene (Sigma) and combined with  $10^6$  targeted cells for 6 h. Cells were infected twice and selected 48 h post-second infection with puromycin (0.5  $\mu\text{g}/\text{ml}$ ), neomycin (100  $\mu\text{g}/\text{ml}$ ) or hygromycin (25  $\mu\text{g}/\text{ml}$ ).

### Soft-agar colony formation assay

To measure anchorage-independent growth, cells were detached with trypsin and resuspended in growth medium. Plates were prepared with a coating of 0.75% low-melting agarose (Lonza) in growth medium and then overlaid with a suspension of cells in 0.45% low-melting agarose ( $5 \times 10^4$  cells/well). Plates were incubated for 3 weeks at 37°C and colonies were counted under microscope. Experiments were performed in triplicate.

### Mouse injection

Eight-week old female athymic *Swiss nude* mice (C. River laboratories) were X-irradiated (4 Gy) prior to injection. Single cell suspensions, ( $5 \times 10^6$  HMEC derivatives resuspended in a PBS-Matrigel (1/1) mixture) were injected into the fat pad of a mammary gland. Tumor incidence was monitored up to 90 days post-injection. Animals were allowed to form tumors up to 1.5 cm in diameter, at which point animals were euthanized. Each tumor was dissected, fixed in paraformaldehyde and processed for histopathology examination.

### Immunoblot analysis

Cells were washed twice with phosphate buffered saline (PBS) containing  $\text{CaCl}_2$  and then lysed in a 100 mM NaCl, 1% NP40,

0.1% SDS, 50 mM Tris pH 8 RIPA buffer supplemented with a complete protease inhibitor cocktail (Roche). Protein expression was examined by western blot using anti-E-cadherin clone 36 (Becton Dickinson), anti- $\beta$ -catenin clone 14 (Becton Dickinson), anti-fibronectin clone 10 (Becton Dickinson), anti-vimentin clone V9 (Dako), anti-N-cadherin clone 32 (Becton Dickinson), anti-occludin clone OC-3F10 (Zymed Laboratories), anti- $\beta$ -actin clone AC-15 (Sigma), anti-HA clone 11 (BabCO), anti-TWIST Twist2C1a (Abcam) monoclonal antibodies and a rabbit polyclonal anti-H-RAS clone C20 (Santa Cruz) for primary detection. Horseradish peroxidase-conjugated rabbit anti-mouse and goat anti-rabbit polyclonal antibodies (Dako) were used as secondary antibodies. Western blots were revealed using an ECL detection kit (Amersham) or a western-blotting Luminol reagent (Santa Cruz).

### Immunofluorescence

$10^4$  cells were seeded on 8-well Lab-TekII chamber slide, fixed in 3% paraformaldehyde (Sigma) and permeabilized in 0.1% Triton 100X (Sigma) in PBS buffer at room temperature for 10 min. The cells were then washed 3 times with PBS and incubated with a blocking solution (10% horse serum in PBS). The cells were then incubated with the anti-E-cadherin clone 36 (Becton Dickinson) or the anti-vimentin clone V9 (Dako) primary antibodies overnight at 4°C. Phalloidin labeling was performed by incubating cells with 1  $\mu\text{g}/\text{ml}$  of TRITC-conjugated Phalloidin P1951 (Sigma) for 30 min. Following extensive washes in PBS, nuclei were stained with Hoechst 5  $\mu\text{g}/\text{ml}$  for 10 min and mounted with Fluoromount-G (SouthernBiotech). All matched samples were photographed (control and test) using an immunofluorescence microscope (Leica) and identical exposure times.

### Immunohistochemistry on murine tumors

The immunohistochemical study was performed on three microns deparaffinized sections, using the avidin-biotin-peroxidase complex technique (LSAB universal, Dako), after 15 min heat-induced antigen retrieval in 10 mM citrate buffer, pH 6. The primary anti-E-cadherin clone 36 diluted at 1/500 (Becton Dickinson), anti-vimentin clone V9 diluted at 1/200 (Dako) and anti-c-MYC A14 at 1/100 (Santa-Cruz Biotechnology) antibodies were applied 60 min at room temperature.

### Immunohistochemistry on xenograft tumors

Paraffin embedded tumors were serially sectioned at a thickness of 4  $\mu\text{m}$ . After deparaffinisation and rehydration, endogenous peroxidases were blocked by incubating the slides in 5% hydrogen peroxide in sterile water. For heat induced antigen retrieval, tissue sections were boiled at 97°C for 40 min either in a 10 mM citrate buffer pH 6 (when anti-cytokeratin and anti-vimentin antibodies were used) or in buffer pH 7 (Dako) (for the anti-E-cadherin antibody) clone 36 (BD Biosciences). Slides were then incubated with the monoclonal pancytokeratin clone AE1/AE3, (Dako), the polyclonal anti-vimentin SC7557 (Santa Cruz) or the monoclonal anti-E-cadherin clone 36 (BD Biosciences) primary antibodies or a non-immune serum used as a negative control, for 1 h at room temperature. Slides were rinsed in phosphate buffered saline, and then incubated with a biotinylated secondary antibody bound to a streptavidin peroxidase conjugate (LSAB+ kit, Dako).

### Microarray analysis

Microarray processing and data analysis as well as procedures to classify human cell lines and mammary tumors are described in detail in Text S1.

### Protein phosphatase activity

Cells were lysed in a 50 mM Tris-HCl (pH 7.5), 150 mM NaCl, 2 mM EDTA, 1 mM EGTA, 0.3% CHAPS lysis buffer supplemented with a protease inhibitor cocktail (Roche) and cleared by centrifugation. The PP2A activity was assessed using the “Serine/Threonine Phosphatase Assay System” (Promega) according to the manufacture instruction. Briefly, the cleared cell lysate was filtered through a Sephadex G25 column to remove free phosphate. Protein concentration was determined using the Bradford method. 5  $\mu$ g of cell protein was incubated in presence of the RRA(pT)VA substrate in a 250 mM imidazole pH 7.2, 1 mM EGTA, 2 mM EDTA, 0.1%  $\beta$ -mercaptoethanol, 0.5 mg/ml BSA PP2A-specific reaction buffer at 25°C for 30 min. After incubation with 50  $\mu$ l of molybdate dye/additive at 25°C for 30 min, optical density was measured at 620 nm. All determinations were performed in triplicate and the absorbance of the reactions was corrected by determining the absorbance of control reactions without phosphoprotein substrate. The PP2A activity was performed in presence of absence of 5 nM of okadaic acid to confirm the specificity of these reaction conditions. The amount of phosphate released (pmol) was calculated from a standard curve (0–2000 pmol) and was normalized with respect to HMEC-hTERT cells.

### Supporting Information

**Figure S1** Mammary tumors developed by WAP-Cre;*K-rasG12D*;*Twist1* mice exhibit a claudin-low gene expression signature. Gene expression profiles of WAP-Cre;*K-rasG12D*;*Twist1*-mouse derived tumors (A, B and C) and of two MMTV-*Neu* tumor-derived murine luminal cell lines were compared. (A) Statistical values of the Pearson’s correlation to the centroids of intrinsic gene clusters are determined according to the 122 reference murine tumors ([13]). MMTV-*Neu* tumor-derived luminal cell lines were used as control luminal cells. (B) The expression of meaningful genes from the claudin-low signature ([13,21]) is shown. Relative transcript abundance with highest expression is labeled in red and with lowest expression is labeled in green, respectively. (TIF)

**Figure S2** Characterization of the RAS+TWIST1 transgenic mouse-derived tumors. Expression analysis of *Twist1/2*, *Zeb1/2*, *Cdh1*, *Vim*, *Cdln3* and *Cdln7* in murine luminal control tumors 1 and 2 and the WAP-Cre;*K-rasG12D*;*Twist1* (named RAS+TWIST) transgenic mouse derived tumors A to D, as assessed by Q-RT-PCR. Gene expression was assessed using the *Hprt1* housekeeping gene as an internal control. The expression level was normalized with respect to murine luminal control tumor 1. (TIF)

**Figure S3** Combined expression of H-RAS<sup>G12V</sup> and EMT-inducing transcription factors provides HMEC cells with a claudin-low gene expression signature. Hierarchical cluster analysis of the established HMEC-derived cell lines using the intrinsic gene clusters determined according to the cell line gene expression data set of Neve and collaborators [21]. The basal A/basal-like cluster is labeled in green, the basal B/claudin-low cluster is labeled in blue and the luminal cluster is labeled in red, HMEC-derived cell lines are labeled in yellow. (TIF)

**Figure S4** Transformed hTERT/RAS HMEC cells display EMT features. (A) Expression analysis of epithelial and mesenchymal markers in HMEC-hTERT cells, in HMEC-hTERT cells transduced with H-RAS<sup>G12V</sup> (HMEC-hTERT/RAS) and in 21

independent HMEC-hTERT/RAS transformed colonies obtained in a soft-agar transformation assay. (B) mRNA expression analysis of EMT-inducing transcription factors (*ZEB1*, *ZEB2*, *TWIST1* and *TWIST2*) as assessed by Q-RT-PCR in the ten colonies still expressing a significant level of E-cadherin. EMT-inducing transcription factor expression was assessed using the *HPRT1* housekeeping gene as an internal control. The expression level was normalized with respect to HMEC-hTERT cells. E: Epithelial, M: Mesenchymal. (TIF)

**Figure S5** The EMT-promoting cytokine TGF $\beta$  cooperates with H-RAS for malignant transformation of HMEC cells. As depicted on top, HMEC cells were sequentially infected with H-RAS<sup>G12V</sup> and immortalized with hTERT. The EpCAM<sup>+</sup> epithelial cell population was sorted out and treated with TGF $\beta$  (2.5 ng/ml) for a three weeks period. EpCAM<sup>-</sup> mesenchymal cells were sorted out. The properties of the epithelial and mesenchymal isogenic cell lines were next compared. The optional step is indicated with brackets. (A) Upper panels: representative photomicrographs of cells obtained by phase-contrast microscopy. Middle panels: E-cadherin and vimentin expression analysis assessed by immunofluorescence. Lower panels: soft agar colony formation assay. Numbers of colonies are indicated  $\pm$  SD of three replicates. (B) Expression analysis of epithelial and mesenchymal markers by western blotting. (C) *TWIST1/2* and *ZEB1/2* endogenous expression as assessed by Q-RT-PCR using the *HPRT1* housekeeping gene as an internal control. The expression level was normalized with respect to the EpCAM<sup>+</sup> sorted out epithelial cells. (TIF)

**Figure S6** Confirmation of p53 pathway inactivation in p53-depleted cells. Expression analysis of p53, as assessed by western blotting (panels A and D) and immunohistochemistry (panels B and E), in hTERT-shcontrol (shRNA scramble) and hTERT-shp53 HMEC derivatives in response to DNA damage induction by adriamycin (+Adriamycin, panels A to C) or after  $\gamma$ -ray ionizing radiation ( $\gamma$ -IR, panels D to F). Expression in non-treated cells (–Adriamycin or – $\gamma$ -IR) were used as controls. (Panels C and F) Cell-cycle distribution analysis before treatment (0 h) or 8 h/32 h post-treatment (8 h+, 32 h+). Cell cycle distribution in absence of treatment (8 h–, 32 h–) is shown. Percentages of cells distributed in the different cell cycle phases are indicated. (TIF)

**Figure S7** *In vitro* transformation assay of primary human mammary epithelial cells. HMEC cells were sequentially depleted of p53 through RNA interference (shp53), infected or not with H-RAS<sup>G12V</sup> and immortalized by hTERT as depicted on top. The optional step is indicated by brackets. (A) Representative photomicrographs of cells obtained by phase contrast microscopy. (B) Transformation potential analysis, assessed by a soft agar colony formation assay. Numbers of colonies are indicated  $\pm$  SD of triplicate experiments. (C) E-cadherin (TRITC), EpCAM (FITC) and vimentin (FITC) expression analysis assessed by immunofluorescence. (D) Cell distribution and antigenic phenotype analysis using the EpCAM antigen. (E) EMT marker expression analysis in transformed colonies as assessed by western blotting. (TIF)

**Figure S8** Separation of the epithelial and mesenchymal subpopulations of the h-TERT-shp53/RAS HMEC derived subpopulations. Cell morphology, cell distribution and the antigenic EpCAM phenotype are shown. (TIF)

**Figure S9** Characterization of the epithelial and mesenchymal hTERT-shp53/RAS HMEC derived subpopulations. (A) Expression analysis of the epithelial E-cadherin and the mesenchymal vimentin markers assessed by immunofluorescence in the sorted cell subpopulations, as indicated. (B) Expression analysis of epithelial and mesenchymal markers by western blotting. (TIF)

**Figure S10** The differential oncogenic potential of mesenchymal and epithelial hTERT-shp53/RAS HMEC-derivatives does not rely on distinct H-RAS<sup>G12V</sup> expression level. Ectopic expression of RAS in epithelial and transformed mesenchymal hTERT-shp53/RAS cells was assessed by Q-RT-PCR using the *36B4* gene as an internal control. The expression level was normalized with respect to hTERT-shp53/RAS epithelial cells. (TIF)

**Figure S11** TGFβ-driven EMT provides hTERT-shp53/RAS HMEC cells with transformation potential, motility and invasive properties. Sequentially, HMEC cells were depleted in p53 (shp53), infected with H-RAS<sup>G12V</sup>, and immortalized with hTERT. The epithelial subpopulation (1) was sorted out by FACS (EpCAM<sup>+</sup> subpopulation) and treated with TGFβ (2.5 ng/ml) for a three weeks period. The resulting mesenchymal population (2) was sorted out by FACS (EpCAM<sup>-</sup> subpopulation). Experimental steps are schematized on top. Characterization of the epithelial and mesenchymal h-TERT-shp53/RAS isogenic cell lines. (A) Cell distribution before and after cell sorting. Percentages of EpCAM<sup>+</sup> or EpCAM<sup>-</sup> cells are indicated. (B) Representative photomicrographs of cells obtained by phase-contrast microscopy. (C) Soft agar colony formation assay. Numbers of colonies are indicated ± SD of triplicate experiments. (D, E) Migratory and invasive properties analyses as assessed by Boyden chamber migration and Matrigel invasion assays, respectively. (F) Expression analysis of epithelial and mesenchymal markers by western blotting. (TIF)

**Figure S12** Transition from p53-depleted H-RAS<sup>G12V</sup>-expressing epithelial cells into mesenchymal cells following ectopic expression of ZEB1 provides cells with a transformation potential. Ectopic expression of ZEB1 in sorted epithelial hTERT-shp53/RAS HMEC cells induced cell commitment to EMT, as indicated by the morphological change (A) the assessment of E-cadherin and vimentin expression by immunofluorescence (B) and the assessment of EMT marker expression by western blotting (D), provides cells with a transformation potential as assessed in a soft-agar colony assay (C). (TIF)

## References

- Yang J, Mani SA, Donaher JL, Ramaswamy S, Itzykson RA, et al. (2004) Twist, a master regulator of morphogenesis, plays an essential role in tumor metastasis. *Cell* 117: 927–939.
- Thiery JP, Aclouge H, Huang RY, Nieto MA (2009) Epithelial-mesenchymal transitions in development and disease. *Cell* 139: 871–890.
- Aclouge H, Adams MS, Fishwick K, Bronner-Fraser M, Nieto MA (2009) Epithelial-mesenchymal transitions: the importance of changing cell state in development and disease. *J Clin Invest* 119: 1438–1449.
- Peinado H, Olmeda D, Cano A (2007) Snail, Zeb and bHLH factors in tumour progression: an alliance against the epithelial phenotype? *Nat Rev Cancer* 7: 415–428.
- Yang J, Weinberg RA (2008) Epithelial-mesenchymal transition: at the crossroads of development and tumor metastasis. *Dev Cell* 14: 818–829.
- Ansieau S, Morel AP, Hinkal G, Bastid J, Puisieux A (2010) TWISTing an embryonic transcription factor into an oncogene. *Oncogene* 29: 3173–3184.
- Morel AP, Lievre M, Thomas C, Hinkal G, Ansieau S, et al. (2008) Generation of breast cancer stem cells through epithelial-mesenchymal transition. *PLoS One* 3: e2888. doi:10.1371/journal.pone.0002888.
- Mani SA, Guo W, Liao MJ, Eaton EN, Ayyanan A, et al. (2008) The epithelial-mesenchymal transition generates cells with properties of stem cells. *Cell* 133: 704–715.
- Vesuna F, Lisok A, Kimble B, Raman V (2009) Twist modulates breast cancer stem cells by transcriptional regulation of CD24 expression. *Neoplasia* 11: 1318–1328.
- Valsesia-Wittmann S, Magdeleine M, Dupasquier S, Garin E, Jallas AC, et al. (2004) Oncogenic cooperation between H-Twist and N-Myc overrides failsafe programs in cancer cells. *Cancer Cell* 6: 625–630.
- Ansieau S, Bastid J, Doreau A, Morel AP, Bouchet BP, et al. (2008) Induction of EMT by twist proteins as a collateral effect of tumor-promoting inactivation of premature senescence. *Cancer Cell* 14: 79–89.
- Ohashi S, Natsuizaka M, Wong GS, Michaylira CZ, Grugan KD, et al. (2010) Epidermal growth factor receptor and mutant p53 expand an esophageal cellular subpopulation capable of epithelial-to-mesenchymal transition through ZEB transcription factors. *Cancer Res* 70: 4174–4184.
- Prat A, Parker JS, Karginova O, Fan C, Livasy C, et al. (2010) Phenotypic and molecular characterization of the claudin-low intrinsic subtype of breast cancer. *Breast Cancer Res* 12: R68.
- Connerney J, Andreeva V, Leshem Y, Mercado MA, Dowell K, et al. (2008) Twist1 homodimers enhance FGF responsiveness of the cranial sutures and promote suture closure. *Dev Biol* 318: 323–334.
- Clark GJ, Der CJ (1995) Aberrant function of the Ras signal transduction pathway in human breast cancer. *Breast Cancer Res Treat* 35: 133–144.

**Figure S13** TWIST1 expression in human breast *in situ* carcinomas. (A) Immunohistochemical analysis of TWIST1 expression in the normal mammary gland. While TWIST1 is not expressed in mammary epithelial cells (arrows 1), the protein is detected in some stromal fibroblasts (arrows 2). (B) TWIST1 expression was analyzed by immunohistochemistry in 34 human ductal carcinomas (DCIS) of the breast. Representative TWIST1 staining of independent samples is shown. TWIST1 protein was detected in 18 of them. Remarkably, in 11 of these cases TWIST1 was homogeneously expressed in the bulk of the lesion even while cancer cells maintained an epithelial phenotype. Top panels: positive samples harbouring a strong and homogenous staining, Middle panels: positive samples harbouring a weak and/or heterogenous staining, Lower panels: negative samples. (C) Analysis of vimentin expression by immunohistochemistry in TWIST1-positive DCIS. Among the 18 TWIST1-positive samples, 6 expressed significant levels of vimentin while maintaining an epithelial phenotype. Arrows 1: vimentin positive epithelial cells. Arrows 2: vimentin negative epithelial cells. Arrow 3: normal myoepithelial cells expressing vimentin. (TIF)

**Text S1** Supplementary Materials and Methods. Text S1 includes details of procedures employed to perform the transcriptional expression analysis, the microarray processing and analysis, the analysis of the p53 pathway functionality, the flow cytometry analysis, the immunohistochemistry on human samples and the assessment of the ectopic *H-RASG12V* expression. (DOC)

## Acknowledgments

The authors are grateful to T. Jacks for providing the Ki-LSL-*K-rasG12D* transgenic mice. We thank Nicolas Nazaret and Séverine Croze for the microarray data analysis. We are also grateful to Christelle Lamblot, Aline-Barbara Salin, Sophie Léon, and Amélie Colombe for their technical assistance.

## Author Contributions

Conceived and designed the experiments: AP SA A-PM GWH. Analyzed the data: AP SA A-PM GWH. Wrote the paper: AP SA. Performed the *in vitro* experiments: A-PM CT FF SC-C JP AT BG. Performed the *in vivo* experiments: GWH IP. Performed the pathological analyses: MD-S IT. Undertook the gene expression profile analysis: AW JL. Generated the Twist1-transgenic mice: DBS. Generated the Zeb expression vectors: GJB.

16. Jackson EL, Willis N, Mercer K, Bronson RT, Crowley D, et al. (2001) Analysis of lung tumor initiation and progression using conditional expression of oncogenic K-ras. *Genes Dev* 15: 3243–3248.
17. Wagner KU, Wall RJ, St-Onge L, Gruss P, Wynshaw-Boris A, et al. (1997) Cre-mediated gene deletion in the mammary gland. *Nucleic Acids Res* 25: 4323–4330.
18. Wagner KU, McAllister K, Ward T, Davis B, Wiseman R, et al. (2001) Spatial and temporal expression of the Cre gene under the control of the MMTV-LTR in different lines of transgenic mice. *Transgenic Res* 10: 545–553.
19. Robinson GW, McKnight RA, Smith GH, Hennighausen L (1995) Mammary epithelial cells undergo secretory differentiation in cycling virgins but require pregnancy for the establishment of terminal differentiation. *Development* 121: 2079–2090.
20. Miyoshi K, Shillingford JM, Le Provost F, Gounari F, Bronson R, et al. (2002) Activation of beta-catenin signaling in differentiated mammary secretory cells induces transdifferentiation into epidermis and squamous metaplasias. *Proc Natl Acad Sci U S A* 99: 219–224.
21. Neve RM, Chin K, Fridlyand J, Yeh J, Baehner FL, et al. (2006) A collection of breast cancer cell lines for the study of functionally distinct cancer subtypes. *Cancer Cell* 10: 515–527.
22. Herschkowitz JI, Simin K, Weigman VJ, Mikaelian I, Usary J, et al. (2007) Identification of conserved gene expression features between murine mammary carcinoma models and human breast tumors. *Genome Biol* 8: R76.
23. Taube JH, Herschkowitz JI, Komurov K, Zhou AY, Gupta S, et al. (2010) Core epithelial-to-mesenchymal transition interactome gene-expression signature is associated with claudin-low and metaplastic breast cancer subtypes. *Proc Natl Acad Sci U S A* 107: 15449–15454.
24. Hennessy BT, Gonzalez-Angulo AM, Stenke-Hale K, Gilcrease MZ, Krishnamurthy S, et al. (2009) Characterization of a naturally occurring breast cancer subset enriched in epithelial-to-mesenchymal transition and stem cell characteristics. *Cancer Res* 69: 4116–4124.
25. Lim E, Vaillant F, Wu D, Forrest NC, Pal B, et al. (2009) Aberrant luminal progenitors as the candidate target population for basal tumor development in BRCA1 mutation carriers. *Nat Med* 15: 907–913.
26. Keller PJ, Arendt LM, Skibinski A, Logvinenko T, Klebba I, et al. (2011) Defining the cellular precursors to human breast cancer. *Proc Natl Acad Sci U S A* 109: 2772–2777.
27. Hoellich KP, O'Brien C, Boyd Z, Cavet G, Guerrero S, et al. (2009) In vivo antitumor activity of MEK and phosphatidylinositol 3-kinase inhibitors in basal-like breast cancer models. *Clin Cancer Res* 15: 4649–4664.
28. Hahn WC, Counter CM, Lundberg AS, Beijersbergen RL, Brooks MW, et al. (1999) Creation of human tumour cells with defined genetic elements. *Nature* 400: 464–468.
29. Elenbaas B, Spirio L, Koerner F, Fleming MD, Zimonjic DB, et al. (2001) Human breast cancer cells generated by oncogenic transformation of primary mammary epithelial cells. *Genes Dev* 15: 50–65.
30. Hahn WC, Dessain SK, Brooks MW, King JE, Elenbaas B, et al. (2002) Enumeration of the simian virus 40 early region elements necessary for human cell transformation. *Mol Cell Biol* 22: 2111–2123.
31. Wong DJ, Foster SA, Galloway DA, Reid BJ (1999) Progressive region-specific de novo methylation of the p16 CpG island in primary human mammary epithelial cell strains during escape from M(0) growth arrest. *Mol Cell Biol* 19: 5642–5651.
32. Eichhorn PJ, Creighton MP, Bernards R (2009) Protein phosphatase 2A regulatory subunits and cancer. *Biochim Biophys Acta* 1795: 1–15.
33. Chen W, Possemato R, Campbell KT, Plattner CA, Pallas DC, et al. (2004) Identification of specific PP2A complexes involved in human cell transformation. *Cancer Cell* 5: 127–136.
34. Hanahan D, Weinberg RA (2011) Hallmarks of cancer: the next generation. *Cell* 144: 646–674.
35. Pallas DC, Shahrik LK, Martin BL, Jaspers S, Miller TB, et al. (1990) Polyoma small and middle T antigens and SV40 small t antigen form stable complexes with protein phosphatase 2A. *Cell* 60: 167–176.
36. Campbell KS, Auger KR, Hemmings BA, Roberts TM, Pallas DC (1995) Identification of regions in polyomavirus middle T and small t antigens important for association with protein phosphatase 2A. *J Virol* 69: 3721–3728.
37. Walter G, Ruediger R (2012) Mouse model for probing tumor suppressor activity of protein phosphatase 2A in diverse signaling pathways. *Cell Cycle* 11: 451–459.
38. Seeling JM, Miller JR, Gil R, Moon RT, White R, et al. (1999) Regulation of beta-catenin signaling by the B56 subunit of protein phosphatase 2A. *Science* 283: 2089–2091.
39. Janssens V, Goris J (2001) Protein phosphatase 2A: a highly regulated family of serine/threonine phosphatases implicated in cell growth and signalling. *Biochem J* 353: 417–439.
40. Spike BT, Wahl GM (2011) p53, Stem Cells, and Reprogramming: Tumor Suppression beyond Guarding the Genome. *Genes Cancer* 2: 404–419.
41. Tran PT, Shroff EH, Burns TF, Thiagarajan S, Das ST, et al. (2012) *Twist1* Suppresses Senescence Programs and Thereby Accelerates and Maintains Mutant *Kras*-Induced Lung Tumorigenesis. *PLoS Genet* 8: e1002650. doi:10.1371/journal.pgen.1002650.
42. Lopez-Novoa JM, Nieto MA (2009) Inflammation and EMT: an alliance towards organ fibrosis and cancer progression. *EMBO Mol Med* 1: 303–314.
43. Desprat N, Supatto W, Pouille PA, Beaurepaire E, Farge E (2008) Tissue deformation modulates twist expression to determine anterior midgut differentiation in *Drosophila* embryos. *Dev Cell* 15: 470–477.
44. Horiguchi K, Shirakihara T, Nakano A, Imamura T, Miyazono K, et al. (2009) Role of Ras signaling in the induction of snail by transforming growth factor-beta. *J Biol Chem* 284: 245–253.
45. Shin S, Dimitri CA, Yoon SO, Dowdle W, Blenis J (2010) ERK2 but not ERK1 induces epithelial-to-mesenchymal transformation via DEF motif-dependent signaling events. *Mol Cell* 38: 114–127.
46. Husemann Y, Geigl JB, Schubert F, Musiani P, Meyer M, et al. (2008) Systemic spread is an early step in breast cancer. *Cancer Cell* 13: 58–68.
47. Klymkowsky MW, Savagner P (2009) Epithelial-mesenchymal transition: a cancer researcher's conceptual friend and foe. *Am J Pathol* 174: 1588–1593.
48. Damonte P, Gregg JP, Borowsky AD, Keister BA, Cardiff RD (2007) EMT tumorigenesis in the mouse mammary gland. *Lab Invest* 87: 1218–1226.
49. Santisteban M, Reiman JM, Asiedu MK, Behrens MD, Nassar A, et al. (2009) Immune-induced epithelial to mesenchymal transition in vivo generates breast cancer stem cells. *Cancer Res* 69: 2887–2895.
50. Chaffer CL, Brueckmann I, Scheel C, Kaestli AJ, Wiggins PA, et al. (2011) Normal and neoplastic nonstem cells can spontaneously convert to a stem-like state. *Proc Natl Acad Sci U S A* 108: 7950–7955.
51. Paranjape AN, Mandal T, Mukherjee G, Kumar MV, Sengupta K, et al. (2011) Introduction of SV40ER and hTERT into mammospheres generates breast cancer cells with stem cell properties. *Oncogene* 30: 1896–1909.
52. Asiedu MK, Ingle JN, Behrens MD, Radisky DC, Knutson KL (2011) TGFbeta/TNF(alpha)-mediated epithelial-mesenchymal transition generates breast cancer stem cells with a claudin-low phenotype. *Cancer Res* 71: 4707–4719.
53. Sarrjo D, Franklin CK, Mackay A, Reis-Filho JS, Isacke CM (2012) Epithelial and mesenchymal subpopulations within normal basal breast cell lines exhibit distinct stem cell/progenitor properties. *Stem Cells* 30: 292–303.
54. Prat A, Perou CM (2011) Deconstructing the molecular portraits of breast cancer. *Mol Oncol* 5: 5–23.
55. van Deurzen CH, Lee AH, Gill MS, Menke-Pluijmers MB, Jager A, et al. (2011) Metaplastic breast carcinoma: tumour histogenesis or dedifferentiation? *J Pathol* 224: 434–437.
56. Herschkowitz JI, Zhao W, Zhang M, Usary J, Murrow G, et al. (2012) Comparative oncogenomics identifies breast tumors enriched in functional tumor-initiating cells. *Proc Natl Acad Sci U S A* 109: 2778–2783.
57. Chang CJ, Chao CH, Xia W, Yang JY, Xiong Y, et al. (2011) p53 regulates epithelial-mesenchymal transition and stem cell properties through modulating miRNAs. *Nat Cell Biol* 13: 317–323.
58. Kim T, Veronese A, Pichiorri F, Lee TJ, Jeon YJ, et al. (2011) p53 regulates epithelial-mesenchymal transition through microRNAs targeting ZEB1 and ZEB2. *J Exp Med* 208: 875–883.
59. Siemens H, Jackstadt R, Hunten S, Kaller M, Menssen A, et al. (2011) miR-34 and SNAIL form a double-negative feedback loop to regulate epithelial-mesenchymal transitions. *Cell Cycle* 10: 4256–4271.
60. Connerney J, Andreeva V, Leshem Y, Muentener C, Mercado MA, et al. (2006) *Twist1* dimer selection regulates cranial suture patterning and fusion. *Dev Dyn* 235: 1345–1357.
61. Brummelkamp TR, Bernards R, Agami R (2002) A system for stable expression of short interfering RNAs in mammalian cells. *Science* 296: 550–553.